Article

An invariant *Trypanosoma vivax* vaccine antigen induces protective immunity

https://doi.org/10.1038/s41586-021-03597-x

Received: 28 January 2020

Accepted: 29 April 2021

Published online: 26 May 2021

Check for updates

Delphine Autheman[1], Cécile Crosnier[1], Simon Clare[2], David A. Goulding[3], Cordelia Brandt[2], Katherine Harcourt[2], Charlotte Tolley[2], Francis Galaway[1], Malhar Khushu[1], Han Ong[1], Alessandra Romero-Ramirez[4], Craig W. Duffy[4], Andrew P. Jackson[4] & Gavin J. Wright[1,5,6,7]✉

Trypanosomes are protozoan parasites that cause infectious diseases, including African trypanosomiasis (sleeping sickness) in humans and nagana in economically important livestock[1,2]. An effective vaccine against trypanosomes would be an important control tool, but the parasite has evolved sophisticated immunoprotective mechanisms—including antigenic variation[3]—that present an apparently insurmountable barrier to vaccination. Here we show, using a systematic genome-led vaccinology approach and a mouse model of *Trypanosoma vivax* infection[4], that protective invariant subunit vaccine antigens can be identified. Vaccination with a single recombinant protein comprising the extracellular region of a conserved cell-surface protein that is localized to the flagellum membrane (which we term 'invariant flagellum antigen from *T. vivax*') induced long-lasting protection. Immunity was passively transferred with immune serum, and recombinant monoclonal antibodies to this protein could induce sterile protection and revealed several mechanisms of antibody-mediated immunity, including a major role for complement. Our discovery identifies a vaccine candidate for an important parasitic disease that has constrained socioeconomic development in countries in sub-Saharan Africa[5], and provides evidence that highly protective vaccines against trypanosome infections can be achieved.

African trypanosomiasis is an infectious disease that is caused by unicellular parasites of the genus *Trypanosoma*, which are transmitted by the bite of an infected tsetse fly. In humans, trypanosome infections cause sleeping sickness: a deadly disease that threatens the lives of millions of people who live in over 30 countries in sub-Saharan Africa[6]. Some species of trypanosome also infect important livestock animals (including cattle, goats and pigs) and cause the wasting disease nagana (animal African trypanosomiasis), which affects the livelihoods of people who rely on these animals for milk, food and draught power[1]. Approximately three million cattle die from this disease every year, which results in an estimated direct annual economic cost of many hundreds of millions of dollars[7] and represents a major barrier for the socioeconomic advancement of many countries in Africa. Nagana is primarily caused by *T. vivax* and *Trypanosoma congolense* and is currently managed with drugs, but resistance is increasing[8]. Previous attempts to develop subunit vaccines against African trypanosome infections have highlighted the difficulties in overcoming the immune evasion strategies that have been evolved by these parasites to enable them to survive in host blood[9]. These strategies include antigenic variation: the serial expression of an abundant allelically excluded variable surface glycoprotein (VSG), and the rapid removal of surface-bound antibodies by hydrodynamic sorting[3,10]. It is widely thought that the VSG forms a constantly changing, impenetrable surface coating that sterically shields other surface proteins from host antibodies, which leads to chronic infections characterized by oscillating parasitaemia; however, a careful analysis of recent structural information suggests that this model may not fully explain the protective role of the VSGs[11]. We therefore hypothesized that the VSGs may also subvert natural immunity by preventing the acquisition of high-titre antibody responses to protective antigens, suggesting that eliciting prophylactic unnatural host immunity by vaccination could be achieved. Here we report the identification of a conserved cell-surface protein that—when used as a subunit vaccine in a mouse model of *T. vivax* infection—is capable of eliciting highly protective immunity.

A subunit vaccine induces immunity to *T. vivax*

To identify subunit vaccine candidates for *T. vivax*, we established a genome-led vaccinology approach using a bioluminescent mouse model of infection[4] (Fig. 1a). We determined that adoptive transfer of about 100 parasites intravenously into BALB/c mouse hosts resulted in an acute, reproducible infection that permitted sensitive and accurate quantification of parasitaemia using light-based imaging[12]. We selected subunit vaccine candidates by searching the *T. vivax* genome[13] for genes that encode predicted cell-surface and secreted proteins that are likely to be accessible to vaccine-elicited antibodies.

[1]Cell Surface Signalling Laboratory, Wellcome Sanger Institute, Hinxton, UK. [2]Pathogen Support Team, Wellcome Sanger Institute, Hinxton, UK. [3]Electron and Advanced Light Microscopy, Wellcome Sanger Institute, Hinxton, UK. [4]Department of Infection Biology and Microbiomes, University of Liverpool, Liverpool, UK. [5]Department of Biology, University of York, York, UK. [6]Hull York Medical School, University of York, York, UK. [7]York Biomedical Research Institute, University of York, York, UK. ✉e-mail: gw2@sanger.ac.uk

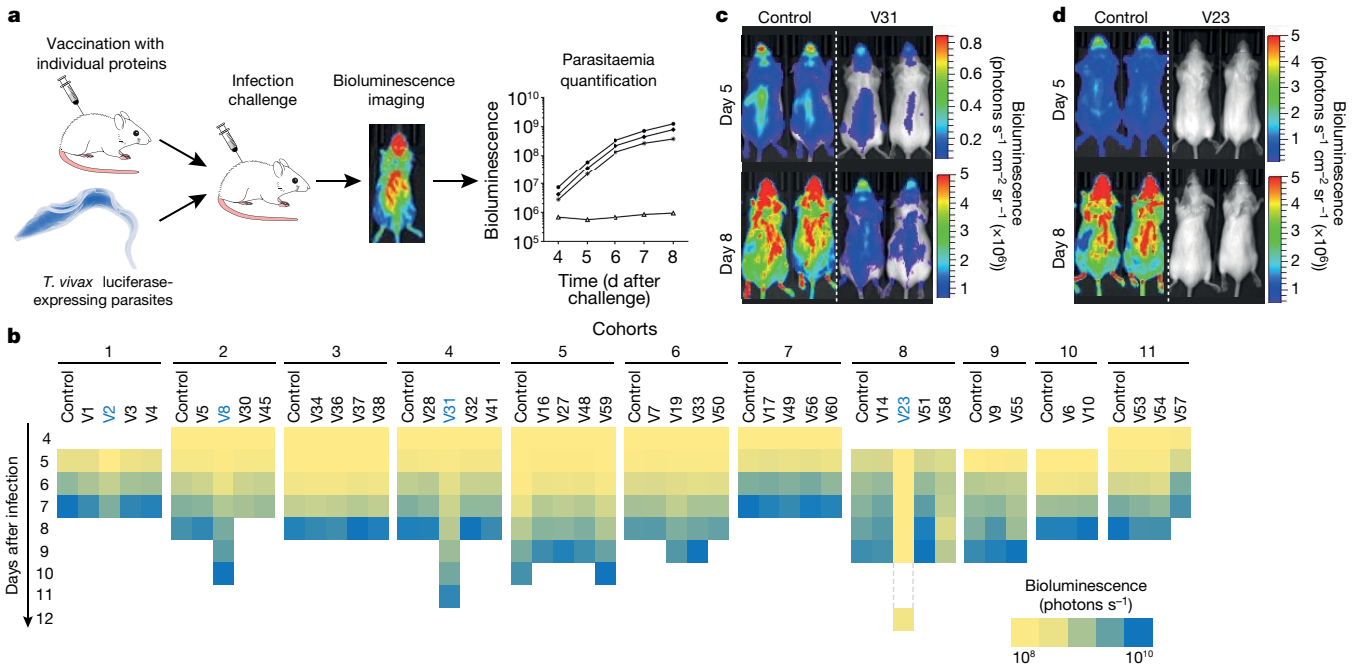

Fig. 1 | Candidate V23 (IFX) induces protective immunity in a mouse model of *T. vivax* infection. a, Schematic of the genome-led vaccinology approach. **b**, Summary of mean parasitaemia ($n \geq 3$ mice) quantified by bioluminescence in cohorts of vaccinated mice challenged with *T. vivax*. Although the V58 candidate had lower mean parasitaemia relative to controls on day 8, it rebounded on day 9 and so was not considered further. **c**, **d**, Bioluminescent images of adjuvant-only control (left panels) and mice vaccinated with V31 (**c** right) and V23 (**d** right); images were taken five (top panels) and eight (bottom panels) days after infection.

We selected 60 candidates using the following criteria: (1) they did not belong to paralogous gene families (to minimize the risk of functional redundancy in different mammalian hosts)[14]; (2) contained more than 300 amino acids in their predicted extracellular region (and so are likely to be accessible at the cell surface); and (3) had evidence of expression in the blood stages[15] (Supplementary Table 1). We synthesized gene sequences encoding the entire predicted extracellular region, and cloned them into a mammalian protein expression plasmid that contained an exogenous secretion peptide and purification tags. We expressed the candidates as soluble recombinant proteins in HEK293 cells to increase the chance that structurally critical posttranslational modifications were appropriately added. Of the 60 expression plasmids we tested, 39 yielded sufficient protein after purification for vaccination trials (Extended Data Fig. 1a). For vaccination, we used a prime and two-boost regime that used alum as an adjuvant to bias host responses towards humoral immunity. To reduce any systemic adjuvant-elicited effects on disease progression, we rested the vaccinated mice for a minimum of four weeks following the final boost before parasite challenge (Extended Data Fig. 1b, c). *Trypanosoma vivax* loses virulence once removed from donor mice, and so, to avoid confounding effects due to the loss of parasite viability during the infection procedure, we ensured that infections were comparable in control mice challenged before and after the vaccinated mice (Extended Data Fig. 1b).

We determined the elicited antibody titres to each antigen, and the vast majority (90%) had mean half-maximal responses at serum dilutions greater than 1:10,000 (Extended Data Fig. 1d). We found that, of the 39 antigens tested, 34 had no effect on the infection parameters relative to controls (Fig. 1b, Extended Data Fig. 2). We observed statistically significant effects on parasite growth with four antigens (Fig. 1b): two candidates (V2 and V8) exhibited a slight delay, and one candidate (V31) showed a longer delay, to the ascending phase of parasitaemia (Fig. 1b, c), and one candidate (V23) showed no detectable parasites in all five vaccinated mice (Fig. 1b, d). For each of the four candidates, we repeated the experiments using independent protein preparations and larger cohorts of mice. The two candidates that induced a slight delay (V2 and V8) did not replicate, and so were not pursued further (Extended Data Fig. 3a). Candidate V31 reduced the rate of parasite multiplication once more and induced improved protection compared to the initial screen so that 9 out of 15 mice survived until day 16 after infection (Extended Data Fig. 3a). V23 vaccination again elicited robust protection, and longitudinal sampling of these mice showed that 10 out of the 15 mice were protected beyond at least day 170 (Extended Data Fig. 3a, b). We dissected protected mice several months after infection, which revealed no detectable extravascular reservoirs of parasites (Extended Data Fig. 4). On the basis of these and subsequent findings, we propose the name 'invariant flagellum antigen from *T. vivax*' (IFX) for the V23 candidate (TvY486_0807240).

IFX localizes to the flagellum

IFX is a previously uncharacterized type-I cell-surface glycoprotein that contains a short (18 amino acid) cytoplasmic region that does not include any known protein domains and has no paralogues (protein sequence identity greater than 25%) within *T. vivax*, nor homologues in other sequenced genomes of *Trypanosoma* species. To begin the functional characterization of IFX, we asked whether it had a specific localization in blood-stage parasites. Immunocytochemistry showed that staining was localized along the length of the flagellum and loosely concentrated in discrete puncta (Fig. 2a). Using immunogold electron microscopy, we found that IFX was enriched at the boundaries of where the flagellum is attached to the cell body; in different sections, these clusters were either unilaterally or bilaterally located (Fig. 2b). In mid-sagittal sections, IFX was located along the length of the flagellum membrane and concentrated in discrete clusters at the points at which the flagellum was in close apposition to the cell membrane; specifically, the gold particles were located between the flagellum and cell body membranes (Extended Data Fig. 5a–f). These data demonstrated that

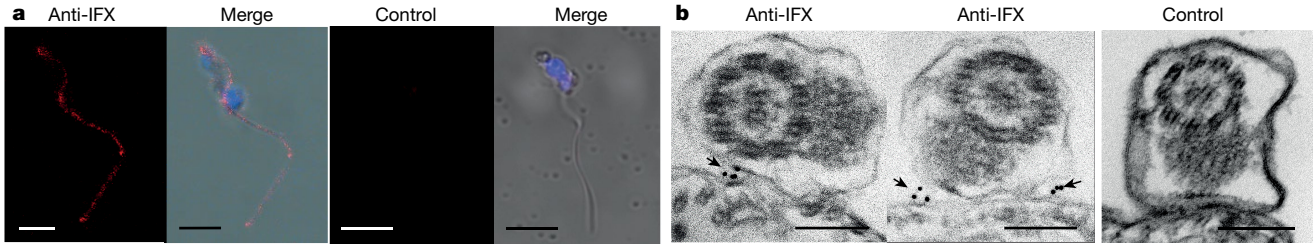

Fig. 2 | IFX is expressed on the flagellum membrane of *T. vivax* and concentrated at the periphery of the flagellum–cell-body contact. **a**, Immunofluorescence staining of *T. vivax* with rabbit anti-IFX antiserum (red) (left) or control pre-immune serum (right) counterstained with DAPI (blue) demonstrates localization of IFX to the flagellum. Scale bars, 5 µm. **b**, Immunogold electron microscopy using an anti-IFX mouse monoclonal antibody localized IFX to the borders of where the flagellum is in contact with the parasite cell body in transverse sections (black arrows in left and middle images) compared to isotype-matched control (right). Scale bars, 100 nm. Representative images of at least two independent experiments are shown.

IFX was localized to the flagellum membrane and particularly enriched as continuous or punctuated bilateral stripes along the flagellum, and bordering the region where the flagellum is attached to the parasite cell body, which suggests a structural role in maintaining flagellar function.

Passive protection by antibodies to IFX

To determine the immunological mechanisms of IFX-mediated protection, we first demonstrated that antibodies contributed to immunity by transferring immune serum from IFX-vaccinated mice to naive recipient mice, which inhibited parasite growth in a dose-dependent manner (Fig. 3a). Depletion of CD4- and CD8-positive T lymphocytes and NK1.1-positive natural killer cells in IFX-vaccinated mice did not affect protective efficacy, demonstrating that these cell types were not direct executors of immunity once it was established (Extended Data Fig. 6). To further investigate the role of antibodies in immunity using an independent approach, we selected six hybridomas that secreted monoclonal antibodies to IFX. Of the six monoclonal antibodies we selected, three affected parasite growth when used in passive protection experiments (Fig. 3b). We determined the approximate location of the monoclonal-antibody-binding sites on IFX and quantified their binding affinities, but did not observe a simple positive correlation between their protective efficacy and either the location of their epitope or binding affinity (Extended Data Fig. 7). The inhibitory effects of one antibody (designated 8E12) titrated with dose (Fig. 3c).

Several mechanisms of anti-IFX protection

Isotyping the monoclonal antibodies to IFX revealed that they were all of the IgG1 subclass, which, in mice, do not effectively recruit immune effector functions such as complement or bind activating Fc receptors with high affinity[16]; this suggests that direct antibody binding to IFX affected parasite viability. To establish the role of Fc-mediated immune effectors in anti-IFX antibody protection, we selected 8E12 (which gave intermediate protective effects) and, by cloning the rearranged antibody variable regions, switched the monoclonal antibody isotype from IgG1 to IgG2a (Extended Data Fig. 8). We observed that the 8E12–IgG2a monoclonal antibodies had a substantially increased potency compared to the 8E12–IgG1 when used in passive transfer experiments (Fig. 4a), and titrating this antibody showed that 3 doses of 50 micrograms or more conferred sterile protection (Fig. 4b, Extended Data Fig. 9a). This demonstrated that the recruitment of antibody-mediated immune effectors was important for parasite neutralization, and to quantify their relative contributions we engineered three further monoclonal antibodies, each of which lacked the binding sites for C1q (ΔC1q), FcRs (ΔFcR) or both (ΔC1qΔFcR)[17] (Extended Data Fig. 8c). When used in passive protection experiments, we observed that mutation of the C1q binding site almost completely reversed the inhibition of parasite growth, which demonstrates that C1q-mediated complement recruitment was a major protective mechanism (Fig. 4c, Extended Data Fig. 9b). Mutating the FcR binding site also relieved the inhibition of

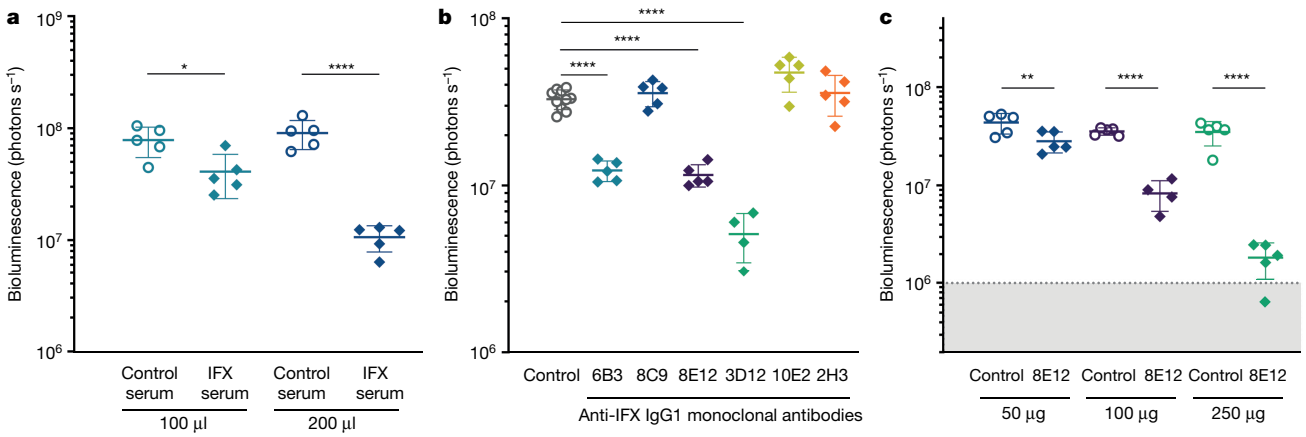

Fig. 3 | Passive transfer of immunity to *T. vivax* infections with anti-IFX antibodies. a, Dose-dependent inhibition of *T. vivax* by adoptive transfer of sera from IFX-vaccinated mice relative to sera from unimmunized control mice. Groups of five mice were compared by one-way analysis of variance (ANOVA) with Sidak post hoc test; $^{*}P \leq 0.05$, $^{****}P \leq 0.0001$. **b**, Three out of six anti-IFX IgG1-isotype monoclonal antibodies (6B3, 8E12 and 3D12), each given at a dose of 3 × 100 µg, passively protect against *T. vivax* infection relative to an isotype-matched control. Groups of five mice were compared by one-way ANOVA with Sidak post hoc test; $^{****}P \leq 0.0001$. **c**, Passive protection of the 8E12–IgG1 monoclonal antibody is dose-dependent. Parasitaemia was quantified at day 5 using bioluminescence. Data points represent individual mice; bars indicate mean ± s.d., groups of five mice were compared by one-way ANOVA with Sidak post hoc test; $^{**}P \leq 0.01$, $^{****}P \leq 0.0001$. The background bioluminescence threshold is indicated by grey shading.

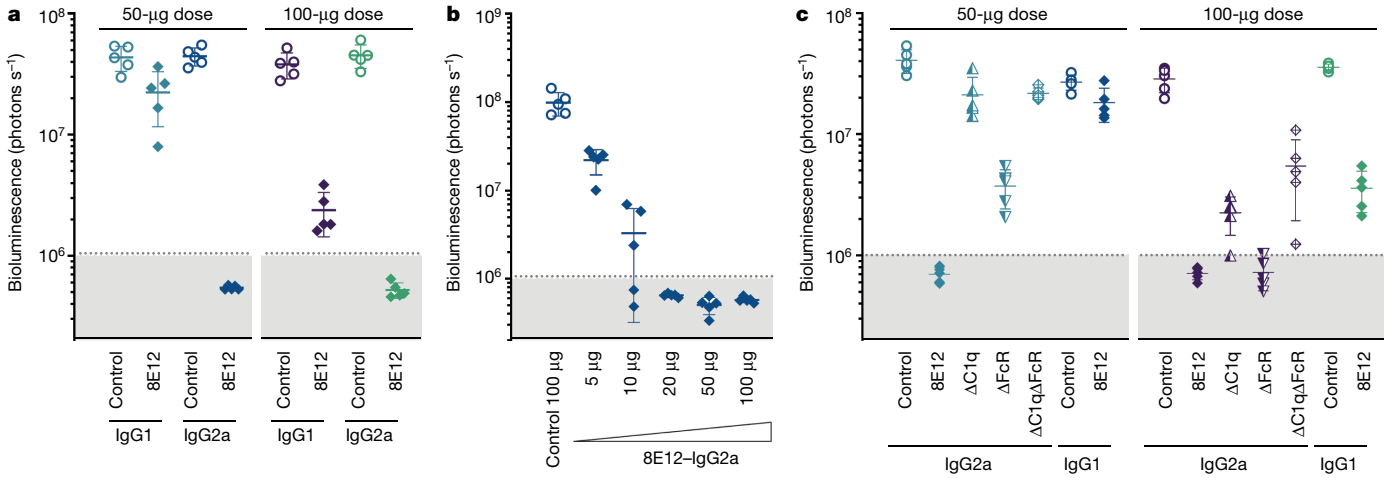

Fig. 4 | There are several mechanisms of antibody-mediated anti-IFX immunological protection, dominated by complement recruitment. **a**, Anti-IFX 8E12–IgG2a monoclonal antibodies passively protect against *T. vivax* infection more potently than do 8E12–IgG1 monoclonal antibodies. **b**, Dose titration of 8E12–IgG2a monoclonal antibody compared to isotype-matched control. **c**, Passive transfer of 8E12–IgG2a monoclonal antibodies containing mutations that prevent binding to C1q (ΔC1q), FcRs (ΔFcR) or both (ΔC1qΔFcR) relieved the inhibition of parasite multiplication to differing degrees, demonstrating that there are several mechanisms of antibody-based immunological protection, including a major role for complement. Parasitaemia was quantified at day 5 using bioluminescence. Data points represent individual mice. Grey shading indicates background bioluminescence. Bars indicate mean ± s.d. One of two independent experiments with very similar outcomes is shown.

parasite growth (but to a lesser extent), whereas mutation of both C1q and FcR sites inhibited growth with a potency similar to that of the IgG1 isotype (Fig. 4c, Extended Data Fig. 9b). These experiments revealed that anti-IFX antibodies inhibited parasite multiplication by several immune mechanisms, dominated by the recruitment of complement.

IFX is highly conserved across isolates

To further assess and develop IFX as a potential vaccine target, we tested appropriate routes of administration and other adjuvants that would bias antibody responses towards more-protective isotypes. Of two selected adjuvants that have previously been used in veterinary vaccines and can be delivered subcutaneously, we found that the saponin-based adjuvant Quil-A elicited consistent antibody titres equivalent to the protective responses induced by alum, of which a large proportion were of the IgG2 isotypes (Extended Data Fig. 10a, b); these mice were potently protected against parasite challenge (Fig. 5a, Extended Data Fig. 10c). One potential challenge with subunit vaccines is that the genes encoding antigens that elicit protective immune responses in natural infections can be subject to diversifying selection, which potentially leads to strain-specific immunity and limits the usefulness of the vaccine[18]. We therefore analysed the *IFX* gene sequence in 29 cosmopolitan *T. vivax* genomes and showed that it is highly conserved by comparison to other surface antigens. We observed only a single non-synonymous polymorphism in 2 out of 29 strains (Fig. 5b) and both of these were heterozygotes; the frequency of the mutation across all strains was therefore very low (0.058), demonstrating that *IFX* is almost completely invariant within the parasite population. This high level of sequence conservation across isolates suggests that the IFX protein is not a target of host immune responses and, consistent with this, sera from naturally infected cattle were not immunoreactive to IFX (Fig. 5c). Finally, a successful vaccine must be able to elicit long-lasting

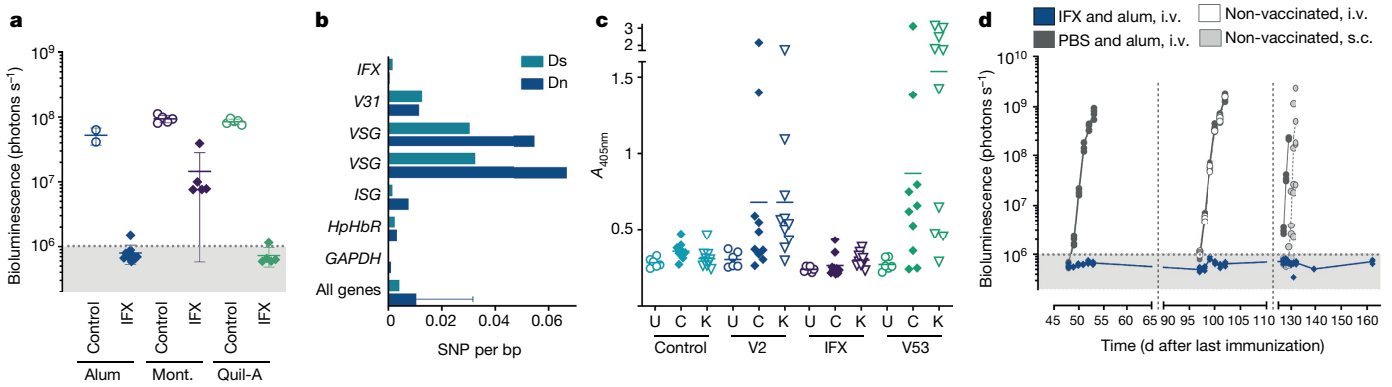

Fig. 5 | IFX is highly conserved and can elicit long-lasting immunity to *T. vivax* infections. **a**, Comparing veterinary adjuvants using subcutaneous delivery demonstrates that Quil-A is as effective as the positive control (IFX adjuvanted in alum and delivered intraperitoneally). Parasitaemia was quantified at day 5 using bioluminescence. Data points represent individual mice. Grey shading indicates background bioluminescence. Bars indicate mean ± s.d. Mont., montanide ISA 201 VG. **b**, Parasite population genetic analysis shows that *IFX* is highly conserved compared to other genes; mean synonymous (Ds) and nonsynonymous (Dn) substitution densities are shown (+s.d. where appropriate). **c**, IFX is not immunogenic in the context of a natural infection. Immunoreactivity to the indicated proteins in sera from Cameroonian (C) ($n = 10$) or Kenyan (K) ($n = 10$) cattle, or uninfected control cattle from the UK (U) ($n = 6$). Bar indicates median. **d**, Mice vaccinated with IFX adjuvanted in alum were protected from two intravenous (i.v.) and one final subcutaneous (s.c.) *T. vivax* challenge given over 100 days after the final booster immunization.

protection: we therefore repeatedly challenged IFX-vaccinated mice over 100 days after they received their final immunization. We observed that mice remained fully protected, including when parasites were delivered subcutaneously (Fig. 5d).

Discussion

We have shown that it is possible to elicit apparently sterile protection to an experimental trypanosome infection with a subunit vaccine that corresponds to the ectodomain of the invariant cell-surface parasite protein IFX. The localization of IFX to the boundaries of where the flagellum is in contact with the parasite cell body suggests it performs a role in flagellar structure and function. Our demonstration that antibodies are required for immunity raises questions about the immunoprotective mechanisms used by trypanosomes, and, importantly, that their vulnerabilities that can be exploited to develop vaccines. The inhibition of parasite growth by antibodies to IFX suggest that the VSG surface coat of *T. vivax* cannot fully shield it from antibody binding, and that anti-IFX antibodies are not removed by endocytosis within the flagellar pocket from the parasite surface with sufficient rapidity to prevent immune effector recruitment mediated by antibodies. The findings that the *IFX* gene sequence was highly conserved across parasite isolates, and that sera from infected cattle living in nagana-endemic regions were not immunoreactive to IFX, suggest that natural parasite infections in some species can subvert host immunity to avoid eliciting protective antibody responses. These mechanisms could include perturbations of the B cell compartment, which have previously been described in experimental models of other trypanosome species[19–21], or that the IFX protein may not be suitably presented to the host immune system in the context of a natural infection. Preliminary experiments to translate these findings to goats did not show protection[22] and highlighted the need to develop infection models that are suitable for vaccine testing, and a greater understanding of which antibody isotypes and adjuvants elicit the necessary mechanisms of immune effector recruitment. The discovery of an antigen that can elicit protection to a trypanosome infection provides optimism and a technical road map that could be followed to identify vaccine antigens not only for other trypanosome species, but also parasites that have thus far proven intractable to vaccine development. Finally, IFX represents a very attractive vaccine candidate for an important livestock disease that has been a major barrier to socioeconomic development in sub-Saharan Africa.

Online content

Any methods, additional references, Nature Research reporting summaries, source data, extended data, supplementary information, acknowledgements, peer review information; details of author contributions and competing interests; and statements of data and code availability are available at https://doi.org/10.1038/s41586-021-03597-x.

1. Morrison, L. J., Vezza, L., Rowan, T. & Hope, J. C. Animal African trypanosomiasis: time to increase focus on clinically relevant parasite and host species. *Trends Parasitol.* **32**, 599–607 (2016).
2. Büscher, P., Cecchi, G., Jamonneau, V. & Priotto, G. Human African trypanosomiasis. *Lancet* **390**, 2397–2409 (2017).
3. Horn, D. Antigenic variation in African trypanosomes. *Mol. Biochem. Parasitol.* **195**, 123–129 (2014).
4. D'Archivio, S. et al. Non-invasive in vivo study of the *Trypanosoma vivax* infectious process consolidates the brain commitment in late infections. *PLoS Negl. Trop. Dis.* **7**, e1976 (2013).
5. Budd, L. T. *DFID-funded Tsetse and Trypanosome Research and Development Since 1980. Vol. 2. Economic Analysis* (DFID Livestock Production, Animal Health and Natural Resources Systems Research Programmes, 1999).
6. Aksoy, S., Buscher, P., Lehane, M., Solano, P. & Van Den Abbeele, J. Human African trypanosomiasis control: achievements and challenges. *PLoS Negl. Trop. Dis.* **11**, e0005454 (2017).
7. Kristjanson, P. M., Swallow, B. M., Rowlands, G. J., Kruska, R. L. & de Leeuw, P. N. Measuring the costs of African animal trypanosomosis, the potential benefits of control and returns to research. *Agric. Syst.* **59**, 79–98 (1999).
8. Tsegaye, B., Dagnachew, S. & Terefe, G. Review on drug resistant animal trypanosomes in Africa and overseas. *Afr. J. Basic Appl. Sci.* **7**, 73–83 (2015).
9. La Greca, F. & Magez, S. Vaccination against trypanosomiasis: can it be done or is the trypanosome truly the ultimate immune destroyer and escape artist? *Hum. Vaccin.* **7**, 1225–1233 (2011).
10. Engstler, M. et al. Hydrodynamic flow-mediated protein sorting on the cell surface of trypanosomes. *Cell* **131**, 505–515 (2007).
11. Schwede, A., Macleod, O. J. S., MacGregor, P. & Carrington, M. How does the VSG coat of bloodstream form African trypanosomes interact with external proteins? *PLoS Pathog.* **11**, e1005259 (2015).
12. Chamond, N. et al. *Trypanosoma vivax* infections: pushing ahead with mouse models for the study of nagana. I. Parasitological, hematological and pathological parameters. *PLoS Negl. Trop. Dis.* **4**, e792 (2010).
13. Jackson, A. P. et al. Antigenic diversity is generated by distinct evolutionary mechanisms in African trypanosome species. *Proc. Natl Acad. Sci. USA* **109**, 3416–3421 (2012).
14. Jackson, A. P. et al. A cell-surface phylome for African trypanosomes. *PLoS Negl. Trop. Dis.* **7**, e2121 (2013).
15. Jackson, A. P. et al. Global gene expression profiling through the complete life cycle of *Trypanosoma vivax*. *PLoS Negl. Trop. Dis.* **9**, e0003975 (2015).
16. Collins, A. M. IgG subclass co-expression brings harmony to the quartet model of murine IgG function. *Immunol. Cell Biol.* **94**, 949–954 (2016).
17. Lo, M. et al. Effector-attenuating substitutions that maintain antibody stability and reduce toxicity in mice. *J. Biol. Chem.* **292**, 3900–3908 (2017).
18. Ouattara, A. et al. Designing malaria vaccines to circumvent antigen variability. *Vaccine* **33**, 7506–7512 (2015).
19. Frenkel, D. et al. *Trypanosoma brucei* co-opts NK cells to kill splenic B2 B cells. *PLoS Pathog.* **12**, e1005733 (2016).
20. Radwanska, M. et al. Trypanosomiasis-induced B cell apoptosis results in loss of protective anti-parasite antibody responses and abolishment of vaccine-induced memory responses. *PLoS Pathog.* **4**, e1000078 (2008).
21. Bockstal, V. et al. *T. brucei* infection reduces B lymphopoiesis in bone marrow and truncates compensatory splenic lymphopoiesis through transitional B-cell apoptosis. *PLoS Pathog.* **7**, e1002089 (2011).
22. Romero Ramirez, A. I. *Antigen Discovery in* Trypanosoma vivax (Univ. Liverpool, 2020).

Methods

A group size of five mice was selected for the initial vaccine screening on the basis of the highly reproducible nature of the *T. vivax* infection between individual mice as quantified by bioluminescence, and the requirement for a strong effect size for an effective vaccine. In a typical vaccine test experiment, we calculate a mean and s.d. of $6 \times 10^7 \pm 1 \times 10^7$ photons per second ($n = 5$) in an adjuvant control cage on day five after infection. A sample size of five mice at 90% statistical power would be sufficient to allow us to detect a reduction in parasitaemia of ≥35% using a one-sided *t*-test at $P \leq 0.05$. Larger group sizes of up to 15 mice were used in replication studies. The experiments were not randomized, and investigators were not blinded to allocation during experiments and outcome assessment, although vaccination and parasite quantification were performed by independent researchers.

Mouse strains and ethical approvals

All mouse experiments were performed under UK Home Office governmental regulations (project licence numbers PD3DA8D1F and P98FFE489) and European directive 2010/63/EU. Research was ethically approved by the Sanger Institute Animal Welfare and Ethical Review Board. Mice were maintained under a 12-h light/dark cycle at a temperature of 19–24 °C and humidity between 40 and 65%. The mice used in this study were 6–14-week-old female *Mus musculus* strain BALB/c, which were obtained from a breeding colony at the Research Support Facility, Wellcome Sanger Institute.

Cell lines and antibodies

Recombinant proteins and antibodies used in this study were expressed in HEK293E[23] or HEK293-6E[24] provided by Y. Durocher. Neither cell line was authenticated but they were regularly tested for mycoplasma (Surrey Diagnostics) and found to be negative. The antibodies used in this study were as follows. Primary antibodies were: six anti-IFX mouse monoclonal antibodies were selected and validated in this study: 6B3, 8C9, 3D12, 2H3, 10E2 and 8E12 from hybridomas that all secreted IgG1 isotypes. A rabbit polyclonal antibody to the entire ectodomain of IFX was generated by Cambridge Research Biochemicals and validated by enzyme-linked immunosorbent assay (ELISA) against the recombinant IFX ectodomain. The 8E12 antibody was cloned and expressed recombinantly as a mouse IgG2a isotype as described in 'Antibody cloning, isotype switching, mutagenesis and purification'. Mouse isotype control antibodies were: IgG1 (MOPC-21, BE0083, BioXcell) and IgG2a (C1.18.4, BE0085, BioXcell). Antibodies used for in vivo leukocyte cell depletion were: anti-mouse CD4 (clone GK1.5, BP0003-1, BioXcell), anti-mouse CD8 (clone 2.43, BP0061, BioXcell), anti-mouse NK1.1 (clone PK136, BE0036, BioXcell), and control anti-keyhole limpet haemocyanin (clone LTF-2, BP0090, BioXcell). Antibodies used for protein quantification for ELISAs were mouse monoclonal anti-His (His-Tag monoclonal antibody, 70796, EMD-Millipore), and biotinylated mouse anti-rat CD4 (clone OX68). OX68 was purified from the spent tissue culture medium from the hybridoma, which was a gift from N. Barclay. Secondary antibodies used were: goat anti-mouse alkaline phosphatase conjugated secondary (A3562, Sigma-Aldrich) and rabbit anti-bovine alkaline phosphatase conjugated secondary (A0705 Sigma-Aldrich). Mouse antibody isotypes were determined using the mouse monoclonal antibody isotyping kit (ISO2-KT Sigma-Aldrich).

Vaccine target identification and expression

The *T. vivax* genome was searched for genes encoding predicted type I, GPI-anchored and secreted proteins using protein feature searching in TriTrypDB[25]. The regions corresponding to the entire predicted extracellular domains of *T. vivax* cell-surface and secreted proteins from the Y486 strain were determined by using transmembrane[26] and GPI-anchor[27] or signal peptide[28] prediction software. Protein sequences encoding the predicted extracellular domain and lacking their signal peptide were codon-optimized for expression in human cells and made by gene synthesis (Geneart and Twist Bioscience). The sequences were flanked by unique NotI and AscI restriction enzyme sites and cloned into a pTT3-based mammalian expression vector[23] between an N-terminal signal peptide to direct protein secretion and a C-terminal tag that included a protein sequence that could be enzymatically biotinylated by the BirA protein–biotin ligase[29] and a 6-His tag for purification[30]. The ectodomains were expressed as soluble recombinant proteins in HEK293 cells as previously described[31,32]. To prepare purified proteins for immunization, between 50 ml and 1.2 l (depending on the level at which the protein was expressed) of spent culture medium containing the secreted ectodomain was collected from transfected cells, filtered and purified by Ni^{2+} immobilized metal-ion affinity chromatography using HisTRAP columns using an AKTAPure instrument (GEHealthcare). Proteins were eluted in 400 mM imidazole as previously described[33], and extensively dialysed into HEPES-buffered saline (HBS) before being quantified by spectrophotometry at 280 nm. Protein purity was determined by resolving one to two micrograms of purified protein by SDS–PAGE using NuPAGE 4–12% Bis Tris precast gels (ThermoFisher) for 50 min at 200 V. Where reducing conditions were required, NuPAGE reducing agent and anti-oxidant (Invitrogen) were added to the sample and the running buffer, respectively. The gels were stained with InstantBlue (Expedeon) and imaged using a c600 Ultimate Western System (Azure biosystems). Purified proteins were aliquoted and stored frozen at −20 °C until used. Where enzymatically monobiotinylated proteins were required to determine antibody titres by ELISA, proteins were co-transfected with a secreted version of the protein biotin ligase (BirA) as previously described[32], and extensively dialysed against HBS and their level of expression determined by ELISA using a mouse monoclonal anti-His antibody (His-Tag monoclonal antibody, 70796, EMD Millipore) as primary antibody and a goat anti-mouse alkaline phosphatase-conjugated secondary (A3562, Sigma-Aldrich).

Vaccine formulation and administration

For the initial screening of antigens, aliquots of purified protein for immunization were thawed, diluted and mixed 50% v/v with alhydrogel adjuvant 2% (InvivoGen) for two hours at room temperature. For each antigen, groups of five 6–8-week-old female BALB/c mice were immunized intraperitoneally using a prime and two-boost strategy using the amounts of protein documented in Supplementary Table 1. For retesting those antigens that had shown some effect in the preliminary screen, one group of 15 mice received three intraperitoneal immunizations of the query protein adjuvanted in alum using similar amounts as used in the initial screen (Supplementary Table 1); a control group, also of 15 mice, received the adjuvant alone. For evaluating different IFX vaccine–adjuvant formulations, groups of five mice received three immunizations of 50 μg IFX adjuvanted with either alhydrogel, montanide ISA 201 VG or Quil-A in a total volume of 200 μl. IFX was formulated with montanide ISA 201 VG according to the manufacturer's instructions using a stirrer to create the water-in-oil emulsion. IFX was mixed in a 1:1 (v/v) ratio with Quil-A adjuvant using a 0.5 mg ml^{-1} solution. IFX adjuvanted in montanide, or Quil-A were administered subcutaneously at two different injection sites (100 μl per site), whereas IFX adjuvanted in alhydrogel was administered intraperitoneally.

Quantification of serum antibody titres by ELISA

To determine the serum antibody responses to immunized proteins, blood biopsies were collected between ten to twelve days after the final immunization from the tail of each mouse and clotted for two hours at room temperature. Cells were removed by centrifugation, the serum collected, supplemented with sodium azide to a final concentration of 2 mM as a preservative and stored at −20 °C until use. Cattle sera were donated from archived material at the University of Liverpool, originally collected from natural *T. vivax* infections in Cameroon (northwest state), and Kenya (western state) where the infection was positively

identified by thick blood smear and the parasite identified as *T. vivax* using the VerY Diag field test.

To determine the antibody titre against an antigen of interest, individual sera were initially diluted 1:1,000 and then six fourfold serial dilutions in PBST and 2% BSA were prepared. These dilutions were pre-incubated overnight at room temperature with 100 μg ml^{-1} of purified rat CD4d3 + 4-BLH protein to adsorb any anti-biotin or His tag antibodies. Sera were transferred to streptavidin-coated ELISA plates on which the biotinylated target antigen was immobilized. To ensure that all anti-tag antibodies were adsorbed, binding of the lowest dilution of antisera was also tested against biotinylated rat CD4d3 + 4-BLH protein similarly immobilized on the ELISA plate to confirm the absence of any anti-tag immunoreactivity[34]. Sera were incubated for one hour at room temperature followed by three washes with PBST before incubating with an anti-mouse IgG secondary antibody conjugated to alkaline phosphatase (Sigma-Aldrich) used as a 1:5,000 dilution for one hour. Following three further washes with PBST, 100 μl of 1 mg ml^{-1} Sigma 104 phosphatase substrate was added and substrate hydrolysis quantified at 405 nm using a plate reader (Spark, Tecan). To quantify immunoreactivity to *T. vivax* antigens in the context of natural infections, cattle sera were diluted 1:800 in PBST and 2% BSA and incubated for two hours at room temperature with biotinylated ectodomains of V2, V53, IFX or control rat CD200, adsorbed on the microtitre plate. Following three washes with PBST, a secondary rabbit anti-bovine IgG antibody (A0705, Sigma-Aldrich) diluted 1:20,000 was incubated for one hour and washed three times with PBST before adding colorimetric phosphatase substrate and acquiring absorbance readings.

Antibody isotyping

Isotyping of the monoclonal antibodies and polyclonal sera responses was performed using the Mouse Monoclonal Antibody Isotyping Kit (ISO2-KT, Sigma-Aldrich), according to the manufacturer's instructions. In brief, the biotinylated ectodomain of the IFX protein was immobilized on a streptavidin-coated plate, incubated with sera diluted 1:1,000 in PBST and 2% BSA or hybridoma supernatants, washed in PBST before adding isotype-specific goat anti-mouse secondary antibodies diluted 1:1,000. Binding was quantified with an alkaline-phosphatase-conjugated rabbit anti-goat tertiary antibody (1:5,000, Sigma-Aldrich) followed by a colorimetric phosphatase substrate, and hydrolysis products quantified by absorbance readings at 405 nm.

Trypanosoma parasite strain and maintenance

A transgenic form of *T. vivax* genetically engineered to ubiquitously express the firefly luciferase enzyme[35] was provided by P. Minoprio. The parental strain of this parasite is the IL1392 line derived from the Y486 strain used for genome sequencing[13] and has previously been fully documented[12]. Parasites were initially recovered from a frozen stabilate by intraperitoneal administration into two BALB/c female mice. Parasites were maintained by weekly serial blood passage in wild-type female BALB/c mice by taking a blood biopsy, quantifying living parasites in PBS and 20 mM D-glucose by microscopy and infecting four naive mice intravenously. During the course of the project, two further aliquots of frozen parasites were thawed and then used for infection challenges: no significant differences in the kinetics of infection were observed. Luciferase-expressing *T. congolense* parasites were a gift from B. Wickstead and C. Gadelha, and were maintained by weekly serial intravenous blood passage in wild-type female BALB/c mice.

Trypanosoma vivax infections

For infection challenges, bloodstream forms of *T. vivax* parasites were obtained from the blood of an infected donor mouse at the peak of parasitaemia, diluted in PBS and 20 mM D-glucose, quantified by microscopy and used to infect mice by intravenous injection. While establishing the infection model in our facility, we observed that the *T. vivax* parasite was labile and gradually lost virulence once removed from living mice. To reduce the possibility of any artefactual protective effects being due to the loss of parasite virulence during the challenge procedure, we screened the protective effects of antigens in a cohort design. Each cohort contained six cages of five mice: four cages contained mice immunized with a different query subunit-vaccine candidate, and the other two cages contained control mice immunized with adjuvant alone. Vaccinated mice were rested for four to eight weeks after the final immunization to mitigate any possible non-specific protective effects elicited by the adjuvant. During the infection procedure, the mice in the control cages were challenged first and last, and the data from the cohort used only if the infections in the control mice from the two cages were comparable. During the infection procedures, parasites were outside of a living mouse for no more than 40 min. Mice were normally challenged by intravenous delivery of 10^2 (cohorts 1–7, 10 and 11) to 10^3 (cohorts 8 and 9) parasites for the initial screening and passive transfer protection experiments, but were also challenged intraperitoneally during the establishment of the model and subcutaneously when investigating the duration of protection. The mice were not randomized between cages and the operator was not blinded to the group condition. Occasionally, individual infected mice within a group unexpectedly exhibited only background levels of bioluminescence, which was attributed to the injected luciferin substrate not distributing from the site of delivery (possibly due to mislocalization of the injection bolus); in these instances, the mice were excluded from the analysis. This occurred 12 times out of 1,650 injections (0.7%) in screening cohorts 3, 5, 6 and 9. Groups were compared using bioluminescence quantification as a proxy for parasitaemia and one-way ANOVA with Dunnett's post hoc test unless specified.

Quantification of *T. vivax* infections by bioluminescent in vivo imaging

The luciferase substrate D-luciferin (potassium salt, Source BioScience) was reconstituted to 30 mg ml^{-1} in Dulbecco's PBS (Hyclone), filter-sterilized (0.22 μm) and stored in aliquots at −20 °C. Aliquots were thawed and administered to animals at a dose of 200 mg kg^{-1}, by intraperitoneal injection ten minutes before bioluminescence acquisitions. The mice were given three minutes of free movement before being anaesthetized with 2.5% isoflurane and placed in the imaging chamber where anaesthesia was maintained for acquisition. An average background bioluminescence measurement was determined by luciferin administration in five female BALB/c mice and calculating the mean whole-body bioluminescence; where appropriate, this value is indicated as a light grey shading on bioluminescence plots. To determine long-term persistence of the parasites in different organs of infected mice, mice were administered with luciferin, imaged and then euthanized with an overdose of anaesthetic. Mice were then perfused with PBS until the perfusion fluid ran clear, the organs dissected, arranged on a Petri dish and bathed in PBS containing 20 mM glucose and 3.3 mg ml^{-1} luciferin for imaging. Emitted photons were acquired by a charge coupled device (CCD) camera (IVIS Spectrum Imaging System, Perkin Elmer). Regions of interest (ROIs) were drawn and total photons emitted from the image of each mouse were quantified using Living Image software version 4.7.4 (Xenogen), the results were expressed as the number of photons s^{-1}. Bioluminescence values were exported and plotted in Prism GraphPad version 8.0.2, which was also used for testing statistical significance where needed. Where necessary, peripheral parasitaemia was quantified by direct microscopic observation as previously described[12]. In brief, five microlitres of blood obtained from the tail vein were appropriately diluted in PBS containing 20 mM glucose and parasite counts were expressed as number of parasites per blood millilitre.

Passive transfer of immunity

To obtain sufficient sera for adoptive transfer experiments, fifty 6–8-week-old female BALB/c mice were immunized intraperitoneally

three times with 20 µg of purified IFX adjuvanted in alum, with each immunization separated by two weeks. Nine days after the final immunization, sera were collected as above, aliquoted and stored at −20 °C until use. For passive transfer experiments, groups of 10-to-14-week-old female BALB/c mice were dosed three times with either sera or purified monoclonal antibodies on three consecutive days; three hours after the second dosing, mice were challenged intravenously with 10^2 *T. vivax* parasites. When using immune serum for passive transfer protection experiments, doses of 100 and 200 µl of sera from either IFX-vaccinated mice or non-immunized control mice were administered. For monoclonal antibodies, the purified antibody was diluted to the required dose in PBS and 200 µl administered intravenously. Control isotypes antibodies used were MOPC-21 for the IgG1 isotype and C1.18.4 for the IgG2a isotype (both from BioXcell). The serum half-life for mouse IgG1 and IgG2a are known to be between 6 and 8 days[36].

In vivo cell depletion

Groups of five mice were immunized three times with 50-µg doses of purified IFX to induce protective immunity to *T. vivax*. To deplete immune mice of defined leucocyte lineages, mice within each group were depleted by intraperitoneal administration of lineage-specific monoclonal antibodies using standard procedures. In brief, natural killer cells were depleted by four injections of 500 µg of the PK136 monoclonal antibody that targets the NK1.1 glycoprotein at days −5, −1, 0 and 2 relative to *T. vivax* challenge. Mouse CD4 and CD8 T lymphocytes were depleted by one intraperitoneal 750-µg injection of the monoclonal antibodies targeting CD4 (clone GK1.5) or CD8 (clone 2.43) receptors, respectively, the day before the infection. The LFT-2 monoclonal antibody (750 µg) was used as an isotype-matched control antibody. Mice were challenged with 10^2 *T. vivax* parasites and parasitaemia quantified was using bioluminescent imaging as described in 'Quantification of *T. vivax* infections by bioluminescent in vivo imaging'.

Trypanosome genomic sequence analysis

To identify whether IFX had any homologues in other *Trypanosome* species, the entire IFX sequence was analysed with Interproscan; this showed that it does not contain any known protein domains other than the predicted N-terminal signal peptide and transmembrane helix. Comparison of the predicted IFX protein sequence with all the other sequenced *Trypanosoma* species genomes in TriTrypDB[25] (https://tritrypdb.org) using tBLASTx returned no reliable matches; moreover, comparison of a hidden Markov model of the IFX protein sequence with all *Trypanosoma brucei, T. congolense* and *Trypanosoma cruzi* proteins using HMMER also produced no matches, demonstrating IFX is unique to *T. vivax*. To confirm that IFX is present in a single copy, the IFX protein sequence was compared with a six-frame translation of the genome sequence using tBLASTn to identify any sequence copies (annotated or not) with >98% amino acid identity typical of allelic variation.

Illumina sequencing reads from 29 clinical strains isolated from Nigeria, Togo, Burkina Faso, The Gambia, Ivory Coast, Uganda and Brazil were mapped to the *T. vivax* Y486 reference sequence using BWA[37] before single-nucleotide polymorphisms (SNPs) were called using the GATK4 analysis toolkit[38]. Insertion and/or deletions (indels) and variant positions with QD < 2.0, FS > 60.0, MQ < 40.0, MQRankSum < −12.5 or ReadPosRankSum < −8.0 were excluded to produce a final list of 403,190 SNPs. Individuals were classified as missing if allele calls were supported by fewer than three reads. Coding SNPs and synonymous or non-synonymous codon alterations were identified by comparison to the reference annotation using a custom Biopython script; pi-values were calculated on a per site basis using vcftools[39]. Genes selected for comparison were *V31* (TvY486_0003730), two VSGs (TvY486_0031620 and TvY486_0040490), *ISG* (TvY486_0503980), *HpHbR* (TvY486_0040690) and the 'housekeeping' gene *GAPDH* (TvY486_1006840).

Electron microscopy

Trypanosoma vivax parasites were resuspended in 1% formalin prepared using freshly dissolved paraformaldehyde in PBS for 30 min (all steps at room temperature), washed three times in PBS, blocked with PBS and glycine followed by 5% fetal calf serum for 30 min and then incubated with a mouse monoclonal antibody to IFX (clone 8E12) for 1 h. After rinsing, the parasites were incubated with goat anti-mouse IgG preadsorbed to 10 nm gold particles (ab27241 Abcam) for 30 min, washed and fixed in a mixture of 2% formalin and 2.5% glutaraldehyde in 0.1 M sodium cacodylate buffer for 30 min. After washing again, the parasites were post-fixed in 1% osmium tetroxide for 30 min, dehydrated in an ethanol series, embedded in epoxy resin and 60-nm ultrathin sections were cut on a Leica UC6 ultramicrotome, contrasted with uranyl acetate and lead citrate and examined on a 120 kV FEI Spirit Biotwin using a Tietz F4.16 CCD camera. The density of anti-IFX gold particle staining was determined by counting the number of gold particles per µm of membrane on both sagittal and transverse sections. Membrane lengths were determined using the segmented line function in ImageJ version 1.45s and a known image scaling factor. To assign dorsal and ventral sectors, a line was drawn across (transverse) or along (sagittal) the flagellum midpoint.

Anti-IFX antibody selection and characterization

To raise polyclonal antisera against IFX, the entire ectodomain of IFX was expressed and purified and injected into rabbits (Cambridge Research Biochemicals). The sera were purified on Hi-Trap Protein G HP columns (GE Healthcare) according to the manufacturer's instructions. Hybridomas secreting monoclonal antibodies to IFX were selected using standard protocols, as previously described[40]. In brief, the SP2/0 myeloma cell line was grown in advanced DMEM/F12 medium (Invitrogen) supplemented with 20% fetal bovine serum, penicillin (100 U ml^{-1}), streptomycin (100 µg ml^{-1}) and L-glutamine (2 mM). Following spleen dissection and dissociation, 10^8 splenocytes were fused to 10^7 SP2/0 myeloma in 50% PEG (PEG 1500, Roche), using standard procedures. The resulting hybridomas were plated over ten 96-well plates and initially grown in advanced DMEM and F12 medium (Invitrogen) supplemented with 20% fetal bovine serum, penicillin (100 U ml^{-1}), streptomycin (100 µg ml^{-1}) and L-glutamine (2 mM) before addition of hypoxanthine–aminopterin–thymidine (HAT) selection medium 24 h after the fusion. After 11 days, hybridoma supernatants were collect to determine the presence of antibodies reacting to the IFX protein using an ELISA-based method, as previously described[40]. Seven wells (2H3, 3D12, 6B3, 8C9, 8E12, 8F10 and 10E2) containing hybridoma colonies secreting antibodies that reacted with IFX, but not to a control protein containing the same purification tags, were identified and cultured for a further four days in HAT-selection medium. Hybridoma cells from each of the positive wells were cloned by limiting dilution over two 96-well plates at a density of 0.5 cells per well and grown in HAT-free SP2/0 conditioned medium. Eleven days later, twelve wells corresponding to each of the seven clones were selected and tested again by ELISA for reactivity to the IFX protein. Hybridoma 8F10 was not successfully cloned but three positive wells from the remaining hybridomas were chosen for a second round of dilution cloning in the conditions described above. After a final test for reactivity to IFX, a single well from each of the positive clones was expanded and adapted to grow in Hybridoma-SFM serum-free medium (Thermo Fisher).

To determine the location of the anti-IFX monoclonal antibody epitopes, subfragments of the IFX ectodomain corresponding to the boundaries of predicted secondary structure (M1–T251, M1–S472, S135–T251 and N442–S535) were designed, produced by gene synthesis and cloned into a mammalian expression plasmid with an enzymatically biotinylated C-terminal tag (Twist Biosciences). Biotinylated proteins

were expressed as secreted recombinant proteins in HEK293 cells as described in 'Vaccine target identification and expression' and dialysed to remove free D-biotin. Biotinylated IFX fragments were immobilized on a streptavidin-coated plate and binding of the six mouse monoclonal antibodies was tested by ELISA and detected with an alkaline-phosphatase-conjugated anti-mouse secondary antibody (Sigma-Aldrich) as previously described[40]. Binding of a rabbit polyclonal antibody raised to the entire ectodomains of IFX (Cambridge Research Biochemicals) was used as a positive control for each of the subdomains, and detected with an alkaline-phosphatase-conjugated anti-rabbit secondary antibody (Jackson Immunoresearch).

For affinity-purification of monoclonal antibodies from hybridoma culture supernatants, spent supernatants were supplemented with 0.1 M sodium acetate, pH 5.0 immediately before purification on a HiTrap Protein G HP 1 mL column (GE Healthcare) using an AKTA pure instrument. Elution was performed in 0.1 M glycine, pH 2.7 followed by immediate neutralization with 1 M Tris-HCl, pH 9.0. Purified antibodies were extensively dialysed against PBS and stored at 4 °C until use. To capture antibodies on streptavidin-coated sensor chips for biophysical interaction analysis, 300 µg of purified monoclonal antibodies were chemically biotinylated using a 20-fold molar excess of sulfo-NHS-biotin (ThermoFisher) for two hours at room temperature; to remove excess biotin the solutions were dialysed against 5 l PBS for 16 h.

Antibody affinity by surface plasmon resonance

Antibody affinities were determined by surface plasmon resonance (SPR) essentially as previously described[41] using a Biacore 8K instrument (GE Healthcare). To measure antibody interaction affinity rather than avidity, between 400 to 600 RU of biotinylated anti-IFX monoclonal antibodies were immobilized on a streptavidin-coated sensor chip prepared using the Biotin CAPture kit (GE Healthcare); a biotinylated mouse monoclonal antibody (OX68) was used as a non-binding control in the reference flow cell. The entire ectodomain of IFX was used as the analyte, which was first purified and resolved by size-exclusion chromatography on a Superdex 200 Increase 10/300 column (GE Healthcare) in HBS-EP (10 mM HEPES, 150 mM NaCl, 3 mM EDTA, 0.05% v/v P20 surfactant) immediately before use in SPR experiments to remove any protein aggregates that might influence kinetic measurements. Increasing concentrations of twofold dilutions of the entire ectodomain of IFX as a soluble analyte were injected at 30 µl min^{-1} for a contact time of 120 s and dissociation of 600 s. Both kinetic and equilibrium binding data were analysed in the manufacturer's Biacore 8K evaluation software version 1.1 (GE Healthcare) and plotted in Prism GraphPad version 8.0.2. All experiments were performed at 37 °C in HBS-EP.

Antibody cloning, isotype switching, mutagenesis and purification

To switch the isotype of the 8E12 anti-IFX monoclonal antibody from IgG1, it was first necessary to amplify the genes encoding the rearranged light and heavy variable regions from the hybridoma; this was performed essentially as previously described[40]. In brief, total RNAs were extracted from the cloned 8E12 hybridoma using the RNAqueous-micro total RNA isolation kit (Ambion) followed by reverse transcription with Superscript III (Thermo Fisher). PCR products encoding the rearranged heavy and light chain regions were individually amplified using sets of degenerate oligonucleotides and then assembled in a subsequent fusion PCR using a linker fragment to create a single PCR product containing both the rearranged light and heavy chains, as previously described[42]. The fusion PCR product was ligated using the NotI and AscI restriction sites into an expression plasmid obtained from Addgene (plasmid no. 114561) in frame with the mouse constant IgG2a heavy chain[43]. Competent *Escherichia coli* were transformed and purified plasmids used in small-scale transfections of HEK293 cells to identify those plasmids encoding functional antibodies as previously described[44].

To perturb the recruitment of immune effectors in the mouse IgG2a recombinant antibody and retain serum half-life, we mutated the C1q and FcR binding sites in the IgG2a constant heavy chain by site-directed mutagenesis as previously described[17]. Mutation to the binding site of Fcγ receptors (ΔFcR) was achieved by introducing the L234A and L235A substitutions using primers FcR sense 5′-GCACCTAACGCTGCAGGTGGACCATCCG-3′ and FcR anti-sense 5′-TGGTCCACCTGCAGCGTTAGGTGCTGGGC-3′. To abrogate C1q binding (ΔC1q), a single amino-acid change P329A was introduced using primers C1q sense 5′-CAAAGACCTCGCTGCGCCCATCGAGAGAACC-3′ and C1q anti-sense 5′-GATGGCGCAGCGAGGTCTTTGTTGTTGACC-3′. In both cases, antibody mutagenesis was achieved by first amplifying 20 ng of an expression vector containing the mouse constant IgG2a heavy chain with each oligonucleotide separately for nine cycles (denaturation for 45 s at 94 °C; annealing for 40 s at 58 °C; elongation for 7 min and 30 s at 72 °C), using the KOD Hot Start DNA polymerase (Merck). Amplification reactions performed with complementary oligonucleotides were then mixed, 0.5 µl KOD Hot Start DNA polymerase was added to the reaction, and the amplification was resumed for a further 18 cycles. At the end of the reaction, half of the PCR reaction was digested with 20 U DpnI enzyme (New England Biolabs), which specifically cleaves methylated strands from the parental plasmid, for 3 h at 37 °C before transforming 5 µl into TOP10 chemically competent bacteria (Invitrogen). Mutations were confirmed in selected clones by DNA sequencing. To generate a double mutant lacking both the C1q and FcR binding sites (ΔC1qΔFcR), site-directed mutagenesis was performed on an expression plasmid containing the FcR mutation, using the set of oligonucleotides designed for C1q mutagenesis. Both single mutants and the double-mutant backbones were doubly digested with NotI and AscI restriction enzymes and the fusion PCR product encoding the variable regions of the 8E12 recombinant antibody cloned into them, plasmids purified and verified by sequencing.

Antibodies were produced by transfecting HEK293 cells with plasmids encoding the recombinant 8E12–IgG2a monoclonal antibody with the wild-type IgG2a heavy chain, single mutants that lacked C1q and FcR binding, and the double mutant. Six days after transfection, the cell culture supernatant was collected and the recombinant antibodies were purified on a HiTrap Protein G HP 1-ml column, according to the manufacturer's instructions as previously described[40].

Reporting summary

Further information on research design is available in the Nature Research Reporting Summary linked to this paper.

Data availability

Annotated *T. vivax* genome data were obtained from TriTrypDB (https://tritrypdb.org). All data generated or analysed during this study are included in this Article, and/or are available from the corresponding author (G.J.W., who can also be contacted at gavin.wright@york.ac.uk) on reasonable request. Source data are provided with this paper.

23. Durocher, Y., Perret, S. & Kamen, A. High-level and high-throughput recombinant protein production by transient transfection of suspension-growing human 293-EBNA1 cells. *Nucleic Acids Res.* **30**, e9 (2002).
24. Loignon, M. et al. Stable high volumetric production of glycosylated human recombinant IFNalpha2b in HEK293 cells. *BMC Biotechnol.* **8**, 65 (2008).
25. Aslett, M. et al. TriTrypDB: a functional genomic resource for the Trypanosomatidae. *Nucleic Acids Res.* **38**, D457–D462 (2010).
26. Sonnhammer, E. L., von Heijne, G. & Krogh, A. A hidden Markov model for predicting transmembrane helices in protein sequences. *Proc. Int. Conf. Intell. Syst. Mol. Biol.* **6**, 175–182 (1998).
27. Eisenhaber, B., Bork, P. & Eisenhaber, F. Prediction of potential GPI-modification sites in proprotein sequences. *J. Mol. Biol.* **292**, 741–758 (1999).
28. Bendtsen, J. D., Nielsen, H., von Heijne, G. & Brunak, S. Improved prediction of signal peptides: SignalP 3.0. *J. Mol. Biol.* **340**, 783–795 (2004).
29. Bushell, K. M., Söllner, C., Schuster-Boeckler, B., Bateman, A. & Wright, G. J. Large-scale screening for novel low-affinity extracellular protein interactions. *Genome Res.* **18**, 622–630 (2008).

30. Sun, Y., Gallagher-Jones, M., Barker, C. & Wright, G. J. A benchmarked protein microarray-based platform for the identification of novel low-affinity extracellular protein interactions. *Anal. Biochem.* **424**, 45–53 (2012).
31. Crosnier, C. et al. A library of functional recombinant cell-surface and secreted *P. falciparum* merozoite proteins. *Mol. Cell. Proteomics* **12**, 3976–3986 (2013).
32. Kerr, J. S. & Wright, G. J. Avidity-based extracellular interaction screening (AVEXIS) for the scalable detection of low-affinity extracellular receptor-ligand interactions. *J. Vis. Exp.* **61**, e3881 (2012).
33. Bartholdson, S. J. et al. Semaphorin-7A is an erythrocyte receptor for *P. falciparum* merozoite-specific TRAP homolog, MTRAP. *PLoS Pathog.* **8**, e1003031 (2012).
34. Crosnier, C. et al. Systematic screening of 96 *Schistosoma mansoni* cell-surface and secreted antigens does not identify any strongly protective vaccine candidates in a mouse model of infection. *Wellcome Open Res.* **4**, 159 (2019).
35. D'Archivio, S. et al. Genetic engineering of *Trypanosoma* (*Dutonella*) *vivax* and in vitro differentiation under axenic conditions. *PLoS Negl. Trop. Dis.* **5**, e1461 (2011).
36. Vieira, P. & Rajewsky, K. The half-lives of serum immunoglobulins in adult mice. *Eur. J. Immunol.* **18**, 313–316 (1988).
37. Li, H. & Durbin, R. Fast and accurate short read alignment with Burrows-Wheeler transform. *Bioinformatics* **25**, 1754–1760 (2009).
38. DePristo, M. A. et al. A framework for variation discovery and genotyping using next-generation DNA sequencing data. *Nat. Genet.* **43**, 491–498 (2011).
39. Danecek, P. et al. The variant call format and VCFtools. *Bioinformatics* **27**, 2156–2158 (2011).
40. Crosnier, C., Staudt, N. & Wright, G. J. A rapid and scalable method for selecting recombinant mouse monoclonal antibodies. *BMC Biol.* **8**, 76 (2010).
41. Zenonos, Z. A. et al. Basigin is a druggable target for host-oriented antimalarial interventions. *J. Exp. Med.* **212**, 1145–1151 (2015).
42. Müller-Sienerth, N., Crosnier, C., Wright, G. J. & Staudt, N. Cloning of recombinant monoclonal antibodies from hybridomas in a single mammalian expression plasmid. *Methods Mol. Biol.* **1131**, 229–240 (2014).
43. Andrews, N. P. et al. A toolbox of IgG subclass-switched recombinant monoclonal antibodies for enhanced multiplex immunolabeling of brain. *eLife* **8**, e43322 (2019).
44. Staudt, N., Müller-Sienerth, N. & Wright, G. J. Development of an antigen microarray for high throughput monoclonal antibody selection. *Biochem. Biophys. Res. Commun.* **445**, 785–790 (2014).

Acknowledgements This research was funded by the Wellcome Trust (grant 206194) and BBSRC (grant BB/S001980/1). A.R.-R. was supported by a PhD studentship funded by FONDECYT-CONCYTEC, the National Council of Science, Technology and Innovation from Peru (grant contract number 001-2016-FONDECYT). We are indebted to Institut Pasteur for providing us with the *T. vivax* luciferase line. We thank Sanger Institute animal technicians for their support with animal work, N. Karp for advice on experimental design, C. Mackenzie for preliminary work on anti-IFX monoclonal antibodies, E. Coomber for help with hybridoma tissue culture, and M. Carrington, L. Morrison and T. Rowan for helpful discussions.

Author contributions D.A. and G.J.W. designed the study. D.A. prepared proteins, and performed immunizations and parasite challenges with help from S.C., C.B., H.O. and K.H. C.C. selected hybridomas, cloned the 8E12 monoclonal antibody, and did the isotype switching, mutagenesis and purification. D.A.G. performed immunogold labelling. C.T. generated hybridomas. F.G. and M.K. performed SPR experiments and analysis. A.R.-R., C.W.D. and A.P.J. provided and analysed *T. vivax* genome sequences and provided sera from infected cattle. D.A. and G.J.W. prepared the manuscript with comments from all co-authors.

Competing interests D.A. and G.J.W. are named inventors on two UK patent applications relating to this research.

Additional information

Supplementary information The online version contains supplementary material available at https://doi.org/10.1038/s41586-021-03597-x.

Correspondence and requests for materials should be addressed to G.J.W.

Peer review information *Nature* thanks Michael Ferguson and the other, anonymous, reviewer(s) for their contribution to the peer review of this work. Peer reviewer reports are available.

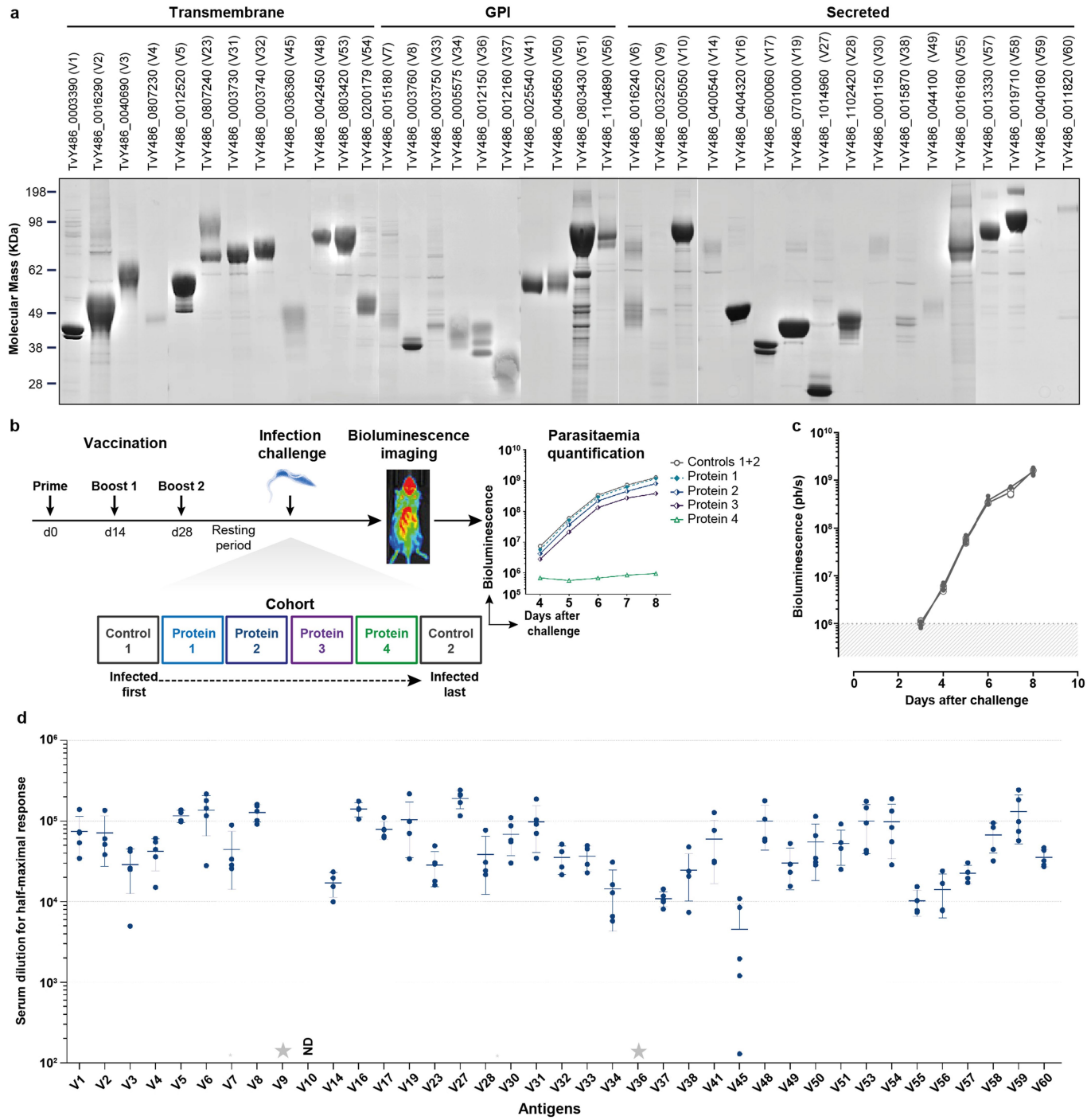

Extended Data Fig. 1 | *Trypanosoma vivax* vaccine candidate antigens, organization of the protection screen and antibody titres. a, Vaccine candidates were expressed as soluble recombinant proteins in HEK293 cells, purified and resolved by SDS–PAGE to determine protein integrity and purity. For uncropped gel images, see Supplementary Fig. 1. **b**, Mice were vaccinated with a protein-in-alum formulation using a prime and two-boost regime and rested before challenge with the luciferase-expressing *T. vivax* parasite line and parasitaemia quantified using bioluminescent imaging. Vaccine candidates were tested in cohorts containing two control cages that were infected first and last to ensure any effect on the reduction of parasite multiplication was not confounded by the loss of parasite virulence. **c**, Parasite multiplication was identical in mice treated with adjuvant alone compared to naive mice. A group of five mice were immunized three times with alum alone (filled circles) and rested for six weeks and the infection with bioluminescent *T. vivax* was compared to naive mice (open circles). Data points represent individual mice; grey shading indicates background bioluminescence. **d**, Serum dilutions for the half-maximal responses for each antigen. Data points are individual mice and bars represent mean ± s.d.; $n = 5$. ND, not determined. Grey stars indicate no detectable response.

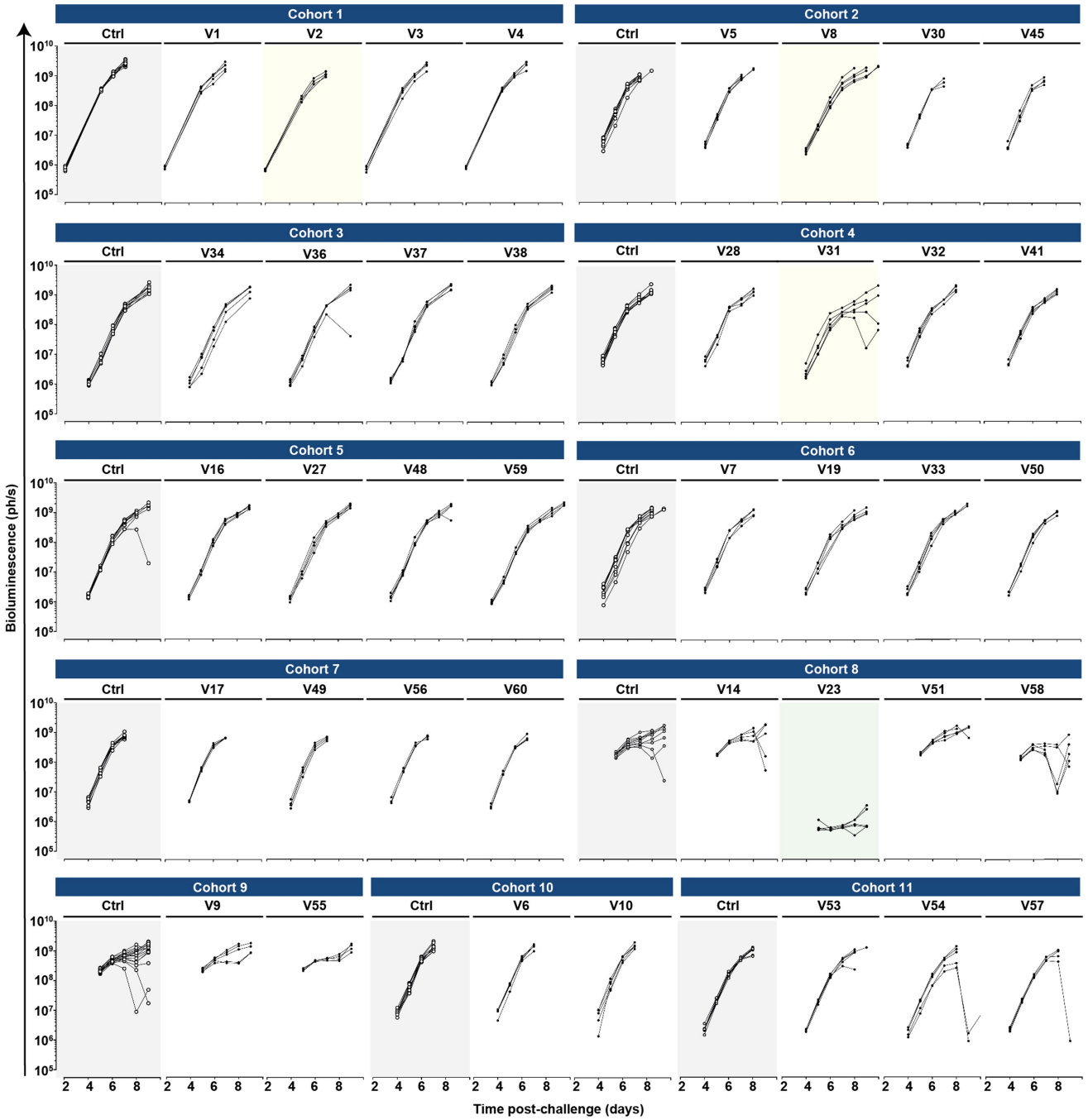

Extended Data Fig. 2 | Summary of systematic genome-led reverse vaccinology screen that identified subunit vaccine candidates for *T. vivax*. Bioluminescence is used as a proxy for parasitaemia and is shown for each mouse in the indicated days post-challenge. Candidates are identified using their 'V number' and organized into their screening cohorts. The two cages of adjuvant-only controls for each cohort are highlighted in grey. The majority of candidates had no effect on the ascending phase of parasitaemia, and are left unshaded. Three candidates (V2, V8 and V31) that had a statistically significant effect on infection are highlighted in pale yellow, and the candidate that elicited strong protection (V23) is highlighted in pale green. Data points are bioluminescence readings from individual mice. The occasional reductions in parasitaemia followed by rebound after day 8 are likely to be due to protective anti-VSG responses and selection of an antigenically distinct variant.

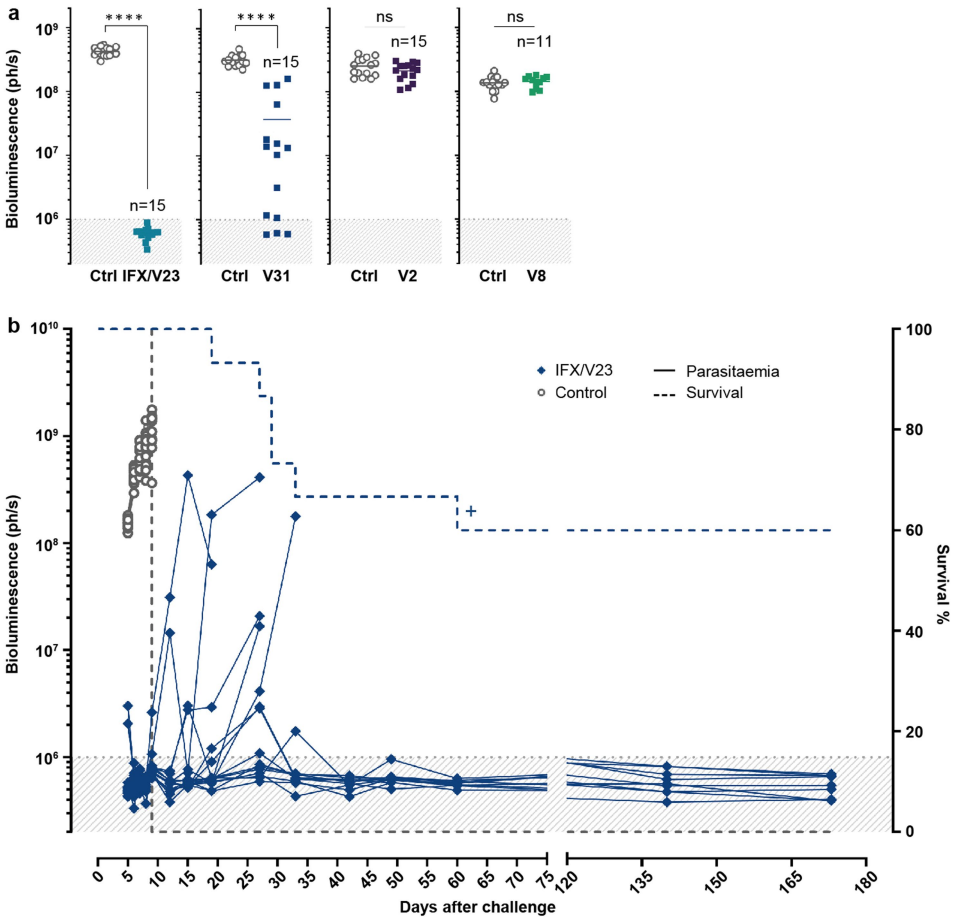

Extended Data Fig. 3 | Replication of strong protective effects in a larger group of mice vaccinated with candidate V23 (IFX). a, Quantification of replicate vaccinations and *T. vivax* infections with four antigens showing protective effects in the initial screen. V23 and V31 vaccinations replicated, but not V2 and V8. Parasitaemia was quantified on day six using bioluminescence; data points represent individual mice and bars indicate mean ± s.d. ns, not significant, $^{****}P \leq 0.0001$ two-tailed *t*-test; grey shading indicates background bioluminescence thresholds. **b**, Fifteen mice were immunized with purified soluble IFX–V23 recombinant protein adjuvanted in alum and challenged with transgenic luciferase-expressing *T. vivax*. Parasitaemia was quantified on the indicated days after parasite challenge using bioluminescence; controls are a cohort of 15 mice treated with adjuvant only. Ten out of the 15 mice were protected until at least day 170. Data points represent individual mice and grey shading indicates bioluminescence thresholds of uninfected mice. Where mice had to be euthanized for health reasons thought to be unrelated to the infection, this is indicated by a cross.

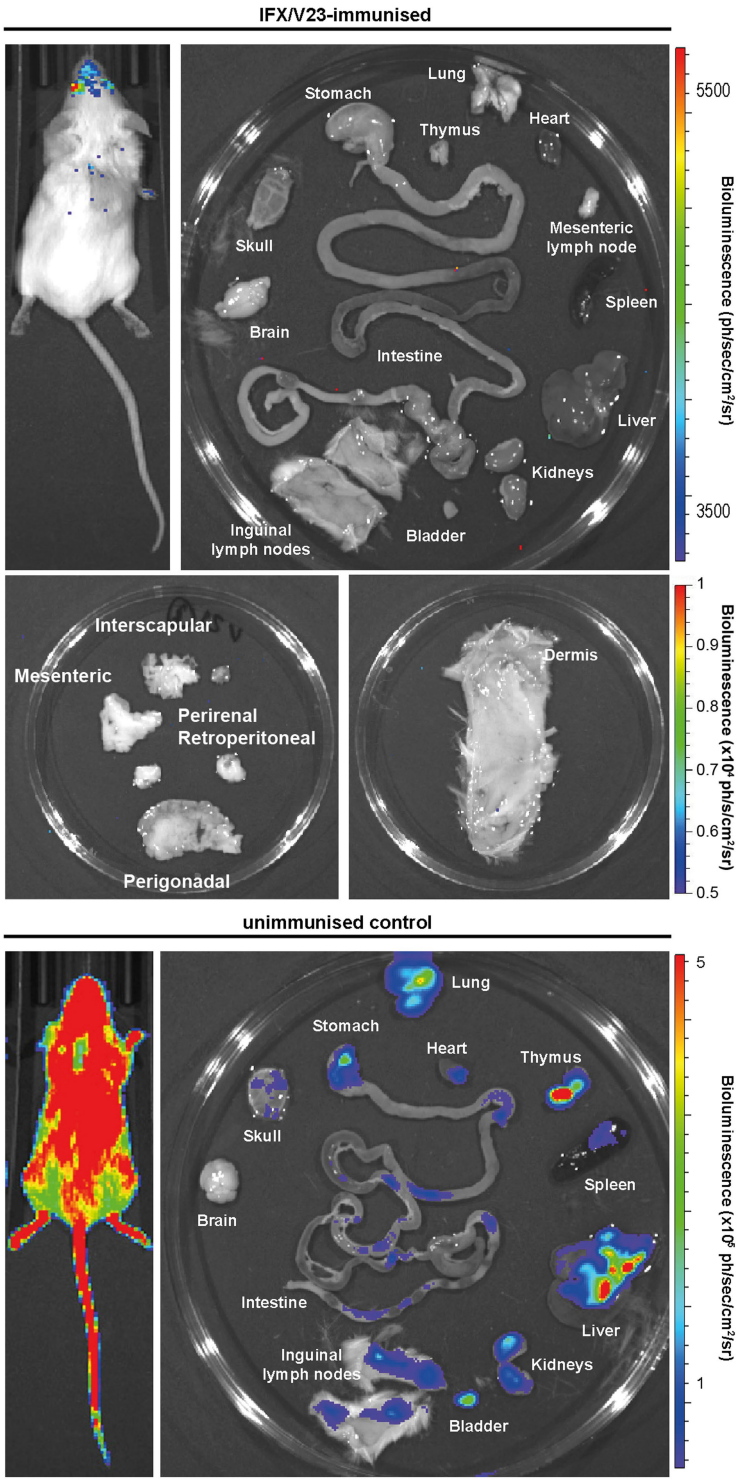

Extended Data Fig. 4 | Parasites do not detectably persist in the organs, adipose tissue or dermis of mice vaccinated with candidate V23 (IFX) challenged with *T. vivax*. An IFX–V23-immunized mouse was challenged with luciferase-expressing transgenic *T. vivax* parasites and protection from infection relative to controls was established. The mouse was rested and, nine months later, injected with luciferin to detect residual parasites using bioluminescence. No bioluminescent signals above background were detected in vaccinated mice either when the whole mouse was imaged, or within the dissected organs, adipose deposits and dermis of IFX–V23-immunized mouse (top panels). An unimmunized mouse was used 8 days after parasite challenge as a positive control (bottom panels).

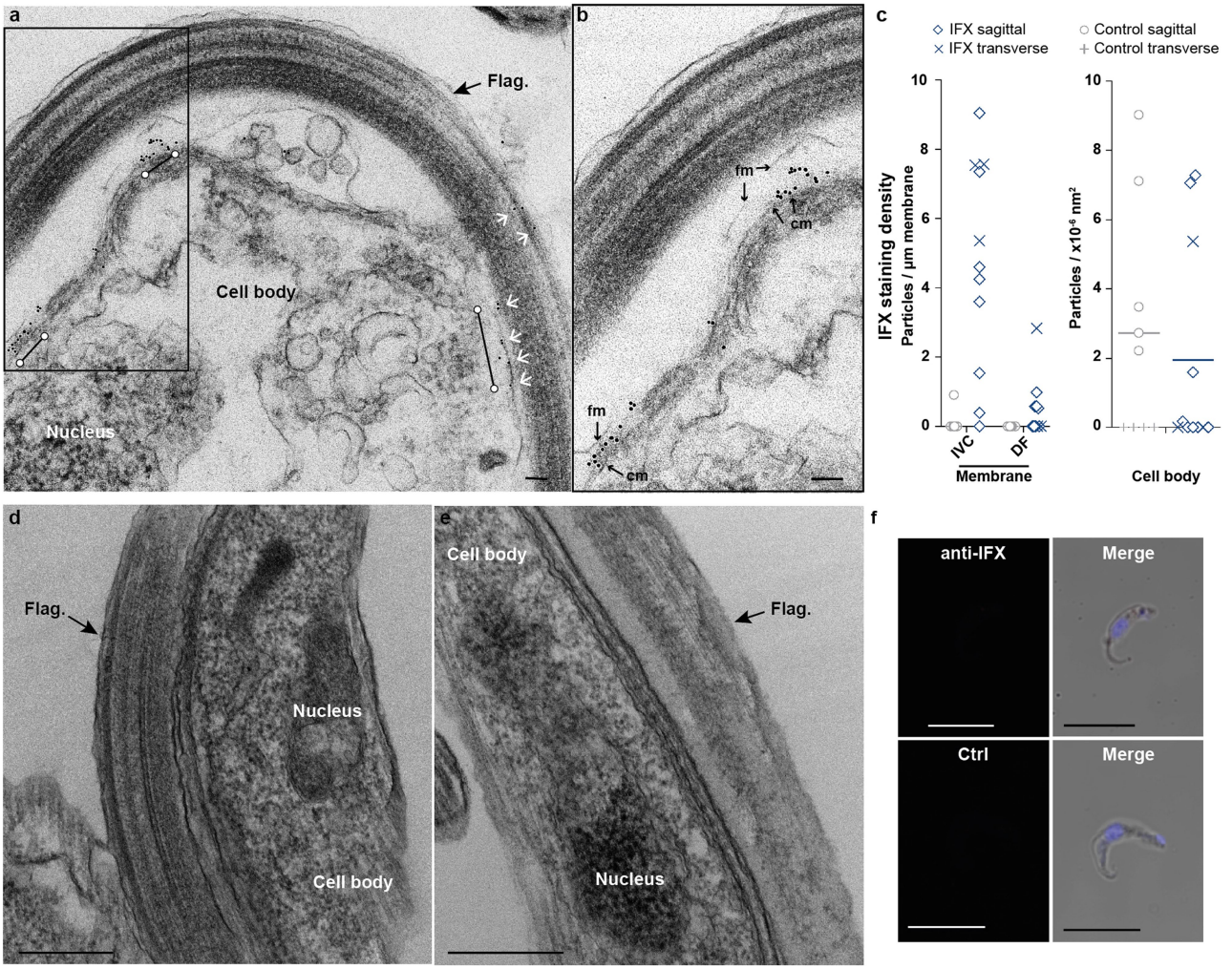

Extended Data Fig. 5 | IFX staining is specific to *T. vivax* and concentrated at the boundary of the flagellum–cell body contact. a, Immunogold electron microscopy using an anti-IFX mouse monoclonal antibody localized IFX to clusters along the length of the flagellum in mid-sagittal sections (white arrows and bars). **b**, Enlarged view of the box in **a**, showing IFX located between the flagellum and cell membranes. **c**, Anti-IFX particle staining density was quantified along the membrane interface of the ventral flagellum–cell body (IVC), dorsal flagellum (DF) and cell body area on sagittal and transverse sections. Individual data points are shown; bars represent means. **d**, **e**, Control electron micrographs of *T. vivax* parasites stained with an isotype-matched control mouse IgG1 antibody (**d**) or goat anti-mouse coated gold particles alone (**e**), showing no accumulation of gold particles. **f**, *Trypanosoma congolense* parasites were stained with anti-IFX rabbit polyclonal sera (top panels) or control preimmune sera (bottom panels) followed by fluorescently conjugated anti-rabbit secondary (red) and counterstained with DAPI (blue). No staining of the parasites was observed demonstrating antibody specificity. Flag., flagellum; fm, flagellar membrane; cm, parasite cell membrane. Scale bars, 100 nm (**a**, **b**), 150 nm (**d**, **e**), 8 µm (**f**). Representative images of at least two independent experiments are shown.

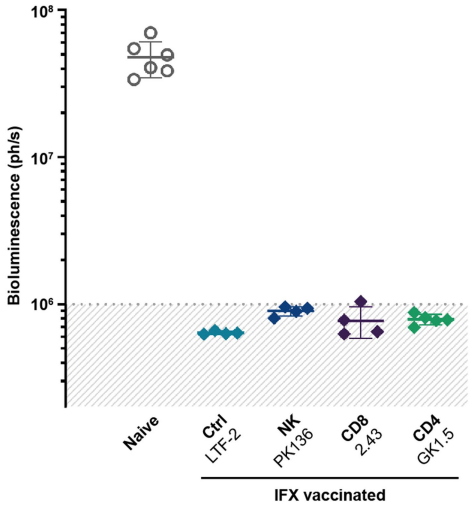

Extended Data Fig. 6 | Depletion of CD4- and CD8-positive T lymphocytes and natural killer cells in IFX-vaccinated mice before parasite challenge do not affect IFX-mediated protective efficacy. Groups of mice were vaccinated with IFX, rested and then either natural killer (NK) cells ($n = 4$) or CD4- ($n = 5$) or CD8-positive ($n = 4$) T lymphocytes were depleted using lineage-specific monoclonal antibodies (antibody clone names indicated) before challenging with luciferase-expressing *T. vivax* parasites. Cell-depleted mice showed no significant difference to control mice treated with an isotype-matched control antibody (LTF-2). The virulence of parasites was confirmed by showing robust infections in naive mice in the same experiment. Parasitaemia was quantified on day 5 using bioluminescence, grey shading indicates bioluminescence thresholds of uninfected mice; data points represent individual mice and bars indicate mean ± s.d.

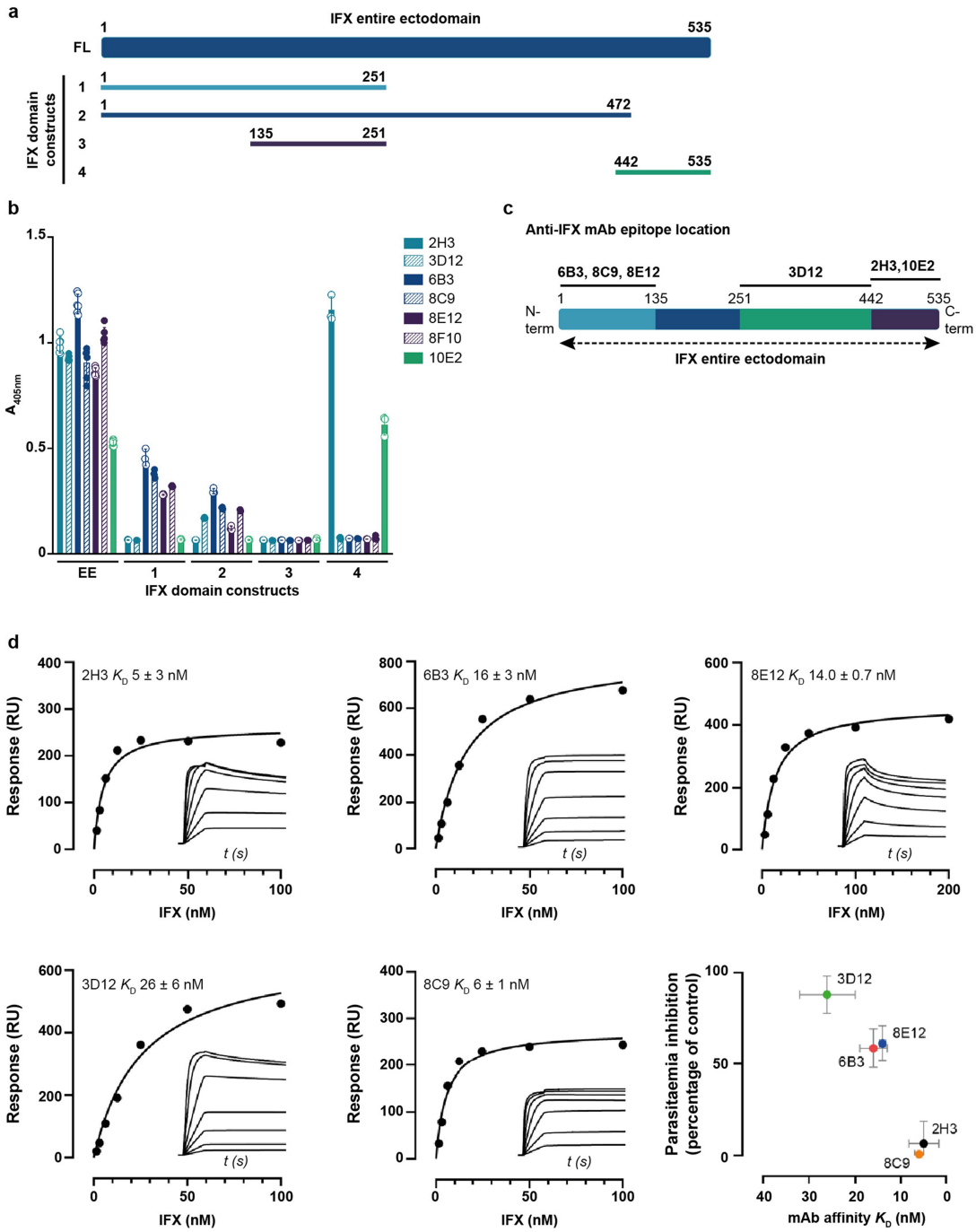

Extended Data Fig. 7 | Identification of the binding epitopes and affinities of a panel of mouse monoclonal antibodies recognizing *T. vivax* IFX. **a**, Schematic showing the N- and C-terminal boundaries of four fragments of the IFX ectodomain. **b**, Identification of the epitope locations for the anti-IFX monoclonal antibodies. The entire ectodomain (EE) ($n = 5$) and derived fragments (1 to 4) ($n = 3$) were expressed as enzymatically biotinylated soluble recombinant proteins in HEK293 cells, immobilized on streptavidin-coated microtitre plates, and the binding of each of the anti-IFX monoclonal antibodies was quantified by ELISA. The hybridoma secreting monoclonal antibody 8F10 was not successfully cloned and therefore not further investigated. Bars represent mean ± s.d. **c**, Schematic of the antibody binding data to the IFX ectodomain fragments, showing the approximate locations of the antibody epitopes. **d**, Quantification of the equilibrium binding affinity of the anti-IFX monoclonal antibodies by SPR. Five of the anti-IFX monoclonal antibodies were chemically biotinylated and immobilized on a streptavidin-coated senor chip and the binding to serial dilutions of purified soluble IFX ectodomains was measured. The binding affinity for each of the antibodies at equilibrium (K_D) was calculated by fitting the binding data (inset) to a simple 1:1 binding isotherm. K_D values are mean ± s.d. using seven analyte dilutions from one experiment. There was no simple positive correlation between the antibody binding affinity and protective efficacy. Antibody affinities were plotted against percentage parasite inhibition in passive transfer experiments at day 5 after infection (mean ± s.d.; $n = 5$).

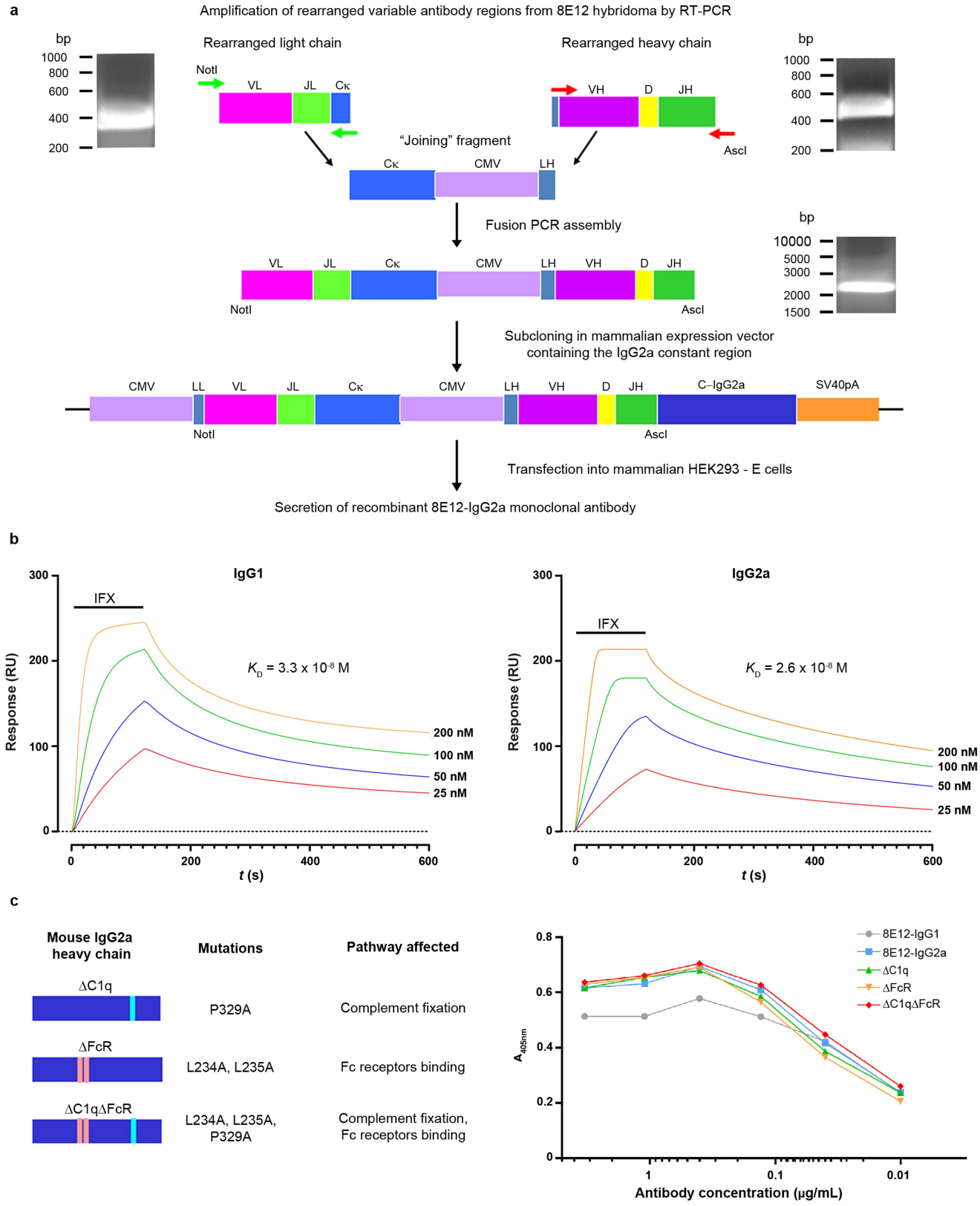

Extended Data Fig. 8 | See next page for caption.

Extended Data Fig. 8 | Recombinant antibody cloning, isotype switching and mutation of antibody effector recruitment sites of the anti-IFX 8E12 hybridoma. a, The rearranged variable light and heavy regions of the anti-IFX 8E12 monoclonal antibody were amplified and assembled by fusion PCR using a 'joining' fragment before being subcloned into a mammalian protein expression plasmid containing the mouse IgG2a heavy chain. Twelve of fifteen colonies expressed functional anti-IFX antibodies and three selected clones contained identical V_H and V_L sequences. The 8E12–IgG2a antibody was produced by transfection of HEK293 cells. For uncropped gel images see Supplementary Fig. 1. **b**, The binding affinity of the 8E12 monoclonal antibody for IFX is unaffected after isotype switching. The biophysical binding parameters of the 8E12 monoclonal antibody for IFX were determined by SPR as both the hybridoma-expressed IgG1 (left) and recombinant IgG2a (right). Serial dilutions of the purified complete ectodomain of IFX were injected for two minutes over the biotinylated antibodies immobilized on a streptavidin-coated sensor chip and left to dissociate. Equilibrium binding constants were calculated by fitting the binding data to a Langmuir binding isotherm and found to be essentially equivalent. **c**, Mutation of the C1q and FcR recruitment sites on the 8E12–IgG2a heavy chain. The specified mutations that are known to abrogate binding to either C1q or FcR were made on the recombinant 8E12–IgG2a plasmid using site-directed mutagenesis. Mutations were made individually (ΔC1q and ΔFcR) and together (ΔC1qΔFcR). Each of the three mutant antibodies were expressed, purified and IFX-binding activity normalized to the parent 8E12–IgG2a and 8E12–IgG1 by ELISA.

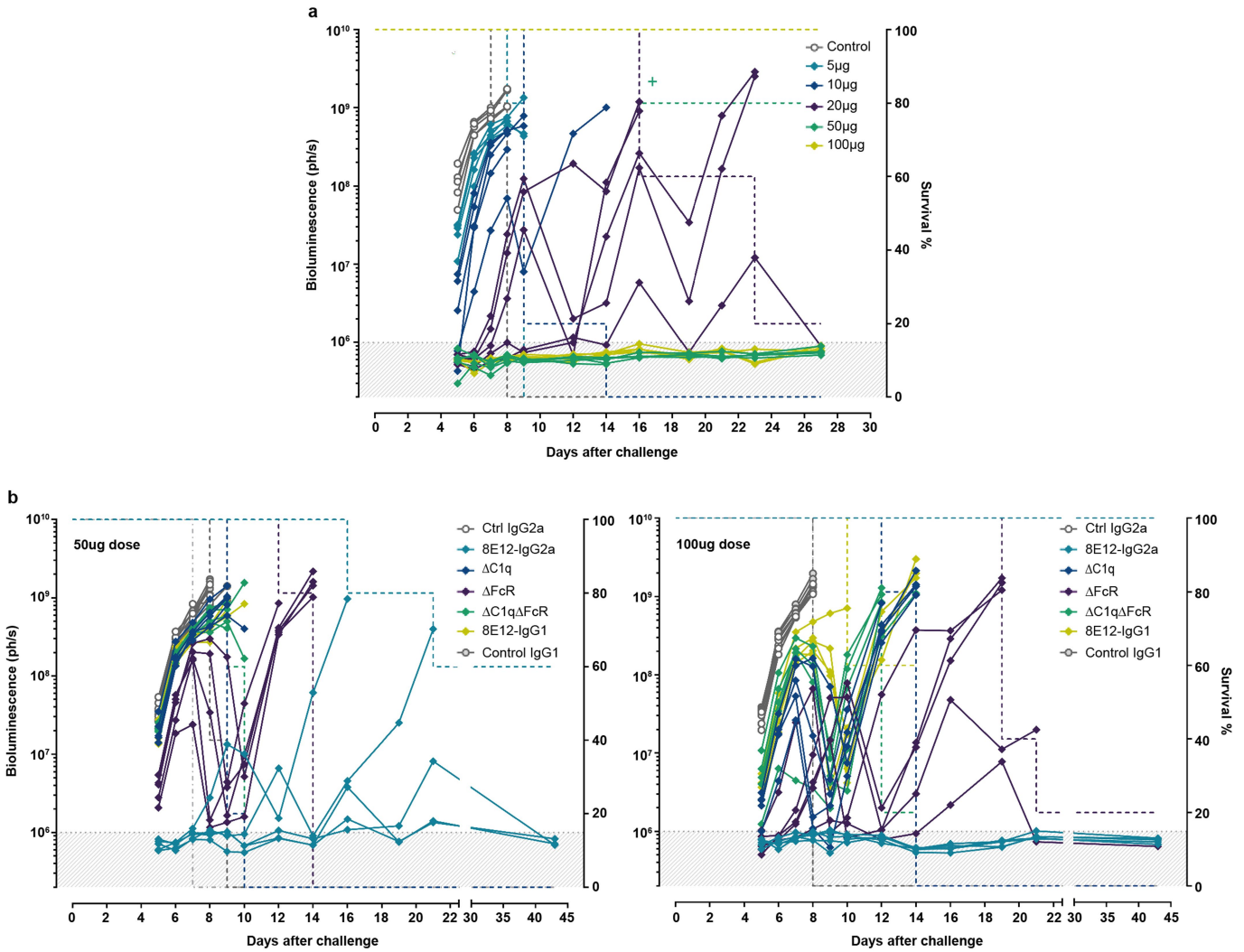

Extended Data Fig. 9 | The anti-IFX 8E12–IgG2a monoclonal antibody with abrogated immune effector recruitment sites reveals highly potent protection due to several mechanisms of immunological protection, including a major role for complement. a, Groups of five mice were injected three times intravenously with the indicated doses of purified anti-IFX 8E12–IgG2a monoclonal antibody and challenged with the luciferase-expressing transgenic *T. vivax* parasites. Control is an isotype-matched mouse IgG2a monoclonal antibody. A cross indicates where a single mouse had to be removed from the study on day 16 for health reasons thought to be unrelated to the infection. **b**, Groups of five mice were administered three times intravenously with either 50 µg (left) or 100 µg (right) of purified anti-IFX 8E12–IgG2a monoclonal antibody containing mutations in immune effector recruitment binding sites and challenged with luciferase-expressing transgenic *T. vivax* parasites. Mutations prevented binding to C1q (ΔC1q), FcRs (ΔFcR) or both (ΔC1qΔFcR) and were compared to non-mutated 8E12–IgG2a, 8E12–IgG1 and both isotype-matched IgG2a and IgG1 controls. In all panels, data points represent individual mice and grey shading indicates bioluminescence thresholds of uninfected mice; dashed lines indicate survival within each group. Reductions in parasitaemia followed by rebounds after day 8 post-infection are likely to be due to the development of protective host antibody responses directed to the dominant VSG within the parasite population and selection of an antigenically distinct variant. One of two independent experiments with very similar outcomes is shown.

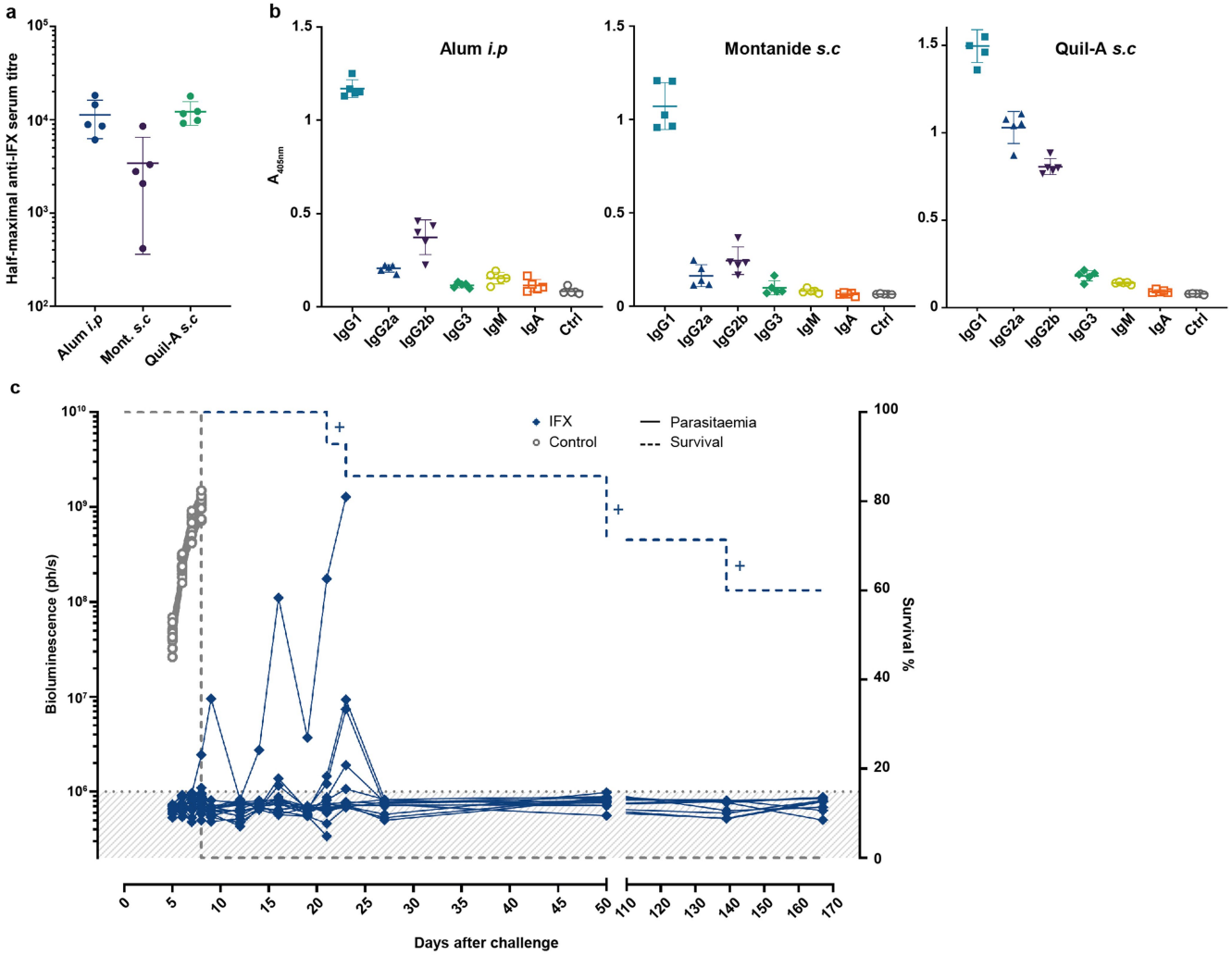

Extended Data Fig. 10 | IFX adjuvanted in Quil-A and delivered subcutaneously induces consistent and isotype-balanced anti-IFX titres that are highly protective. a, Groups of five mice were immunized with the purified ectodomain of IFX adjuvanted in alum, Quil-A and montanide ISA 201 VG (mont.) using a prime and two-boost regime either intraperitoneally (alum i.p.) or subcutaneously (Quil-A and montanide s.c.). Half-maximal anti-IFX titres were determined by ELISA. Bars are mean ± s.d. IFX adjuvanted with Quil-A administered subcutaneously were able to elicit anti-IFX antibody titres that were as high as those elicited by IFX adjuvanted with alum delivered intraperitoneally. **b**, Quantification of different anti-IFX antibody isotypes elicited by the different adjuvants. IFX and Quil-A were able to induce a larger proportion of IgG2 isotype subclasses. Data points represent individual mice ($n = 5$) and bars are mean ± s.d. **c**, Increased protection to *T. vivax* challenge using Quil-A in a protein-in-adjuvant vaccine formulation. Fourteen mice were immunized subcutaneously with purified soluble IFX recombinant protein adjuvanted in Quil-A and challenged with transgenic luciferase-expressing *T. vivax*. Parasitaemia was quantified on the indicated days after parasite challenge using bioluminescence; controls are a cohort of 14 mice treated with adjuvant only. Data points represent individual mice and grey shading indicates bioluminescence thresholds of uninfected mice. Crosses indicate where individuals had to be removed from the study for health reasons thought to be unrelated to the infection. The smaller bioluminescence peaks in four mice corresponding to high bioluminescent readings between days 16 and 24 were caused by bleed-through of bioluminescence signal from the mouse that eventually succumbed to infection.

nature research

Corresponding author(s): Gavin J. Wright

Last updated by author(s): Apr 13, 2021

Reporting Summary

Nature Research wishes to improve the reproducibility of the work that we publish. This form provides structure for consistency and transparency in reporting. For further information on Nature Research policies, see Authors & Referees and the Editorial Policy Checklist.

Statistics

For all statistical analyses, confirm that the following items are present in the figure legend, table legend, main text, or Methods section.

n/a	Confirmed
☐	☒ The exact sample size (*n*) for each experimental group/condition, given as a discrete number and unit of measurement
☐	☒ A statement on whether measurements were taken from distinct samples or whether the same sample was measured repeatedly
☐	☒ The statistical test(s) used AND whether they are one- or two-sided *Only common tests should be described solely by name; describe more complex techniques in the Methods section.*
☒	☐ A description of all covariates tested
☐	☒ A description of any assumptions or corrections, such as tests of normality and adjustment for multiple comparisons
☐	☒ A full description of the statistical parameters including central tendency (e.g. means) or other basic estimates (e.g. regression coefficient) AND variation (e.g. standard deviation) or associated estimates of uncertainty (e.g. confidence intervals)
☐	☒ For null hypothesis testing, the test statistic (e.g. *F*, *t*, *r*) with confidence intervals, effect sizes, degrees of freedom and *P* value noted *Give P values as exact values whenever suitable.*
☒	☐ For Bayesian analysis, information on the choice of priors and Markov chain Monte Carlo settings
☒	☐ For hierarchical and complex designs, identification of the appropriate level for tests and full reporting of outcomes
☒	☐ Estimates of effect sizes (e.g. Cohen's *d*, Pearson's *r*), indicating how they were calculated

Our web collection on statistics for biologists contains articles on many of the points above.

Software and code

Policy information about availability of computer code

Data collection	Bioluminescence data were collected using an in vivo imaging "Spectrum" imaging system. Surface plasmon resonance data were collected on a BIAcore 8K instrument. ELISA data (light absorbance) were collected on an Tecan "Spark" plate reader.
Data analysis	Bioluminescence data were analysed using the custom Living Image software version 4.7.4, bioluminescence values were exported and plotted in Prism GraphPad version 8.0.2 which was also used for tests of statistical significance where needed. Surface plasmon resonance data were analysed using the BIAcore 8K evaluation software version 1.1 and plotted in Prism GraphPad version 8.0.2. Antibody affinity data were obtained using non-linear hyperbola curve fitting to a simple 1:1 binding model. Gold micrograph density analysis was performed using ImageJ software version 1.45s.

For manuscripts utilizing custom algorithms or software that are central to the research but not yet described in published literature, software must be made available to editors/reviewers. We strongly encourage code deposition in a community repository (e.g. GitHub). See the Nature Research guidelines for submitting code & software for further information.

Data

Policy information about availability of data

All manuscripts must include a data availability statement. This statement should provide the following information, where applicable:

- Accession codes, unique identifiers, or web links for publicly available datasets
- A list of figures that have associated raw data
- A description of any restrictions on data availability

Annotated T. vivax genome data were obtained from TriTrypDB (https://tritrypdb.org). All data generated or analyzed during this study are included in this published article and/or available from the corresponding author on reasonable request.

Field-specific reporting

Please select the one below that is the best fit for your research. If you are not sure, read the appropriate sections before making your selection.

☒ Life sciences ☐ Behavioural & social sciences ☐ Ecological, evolutionary & environmental sciences

For a reference copy of the document with all sections, see nature.com/documents/nr-reporting-summary-flat.pdf

Life sciences study design

All studies must disclose on these points even when the disclosure is negative.

Sample size	Group sizes of five animals were selected for the initial vaccine screening based on the highly reproducible nature of the T. vivax infection between individuals as quantified by bioluminescence, and the requirement for a strong effect size for an effective vaccine. In a typical vaccine test experiment for T. vivax, we calculate a mean and standard deviation of 6 x10^7 ± 1 x10^7 photons / sec (n = 5) in an adjuvant control cage on day five after infection. We can calculate that a sample size of 5 animals at 90% statistical power would be sufficient to allow us to detect a reduction in parasitaemia of ≥35% using a one-sided t-test at P ≤ 0.05. Larger groups sizes of up to 15 animals were used in replication studies.
Data exclusions	Occasionally, individual mice within a group unexpectedly exhibited only background levels of bioluminescence at certain time points which was attributed to the injected luciferin substrate not distributing from the site of injection, possibly due to mislocalization of the injection bolus; in these instances, these animals were excluded from the analysis. This occurred 12 times out of 1650 injections (0.7%) in screening cohorts 3, 5, 6, and 9 (Fig.1b).
Replication	Replication studies were performed as described in the text, usually using a larger number of animals. For passive protection experiments, all studies replicated, and a representative experiment of at least two independent experiments is shown. Vaccination experiments showing protective effects were all replicated with larger group size, and vaccination with IFX/V23 and V31 replicated as shown in Extended Data figure 3a.
Randomization	The animals were distributed to their groups based on their age.
Blinding	Pilot experiments where group conditions were blinded were performed but resulted in mixing of protein vaccine administration. Where possible vaccination of the mice and parasite quantification after challenge were performed by independent researchers.

Reporting for specific materials, systems and methods

We require information from authors about some types of materials, experimental systems and methods used in many studies. Here, indicate whether each material, system or method listed is relevant to your study. If you are not sure if a list item applies to your research, read the appropriate section before selecting a response.

Materials & experimental systems

n/a	Involved in the study
☐	☒ Antibodies
☐	☒ Eukaryotic cell lines
☒	☐ Palaeontology
☐	☒ Animals and other organisms
☒	☐ Human research participants
☒	☐ Clinical data

Methods

n/a	Involved in the study
☒	☐ ChIP-seq
☒	☐ Flow cytometry
☒	☐ MRI-based neuroimaging

Antibodies

Antibodies used	Primary antibodies: six anti-IFX mouse monoclonal antibodies were selected and validated in this study: 6B3, 8C9, 3D12, 2H3, 10E2 and 8E12 from hybridomas all secreting IgG1 isotypes. A rabbit polyclonal antibody to the entire ectodomain of IFX was generated by Cambridge Research Biochemicals and validated by ELISA against the recombinant IFX ectodomain. The 8E12 antibody was cloned and expressed recombinantly as a mouse IgG2a isotype. Mouse isotype control antibodies were: IgG1 (MOPC-21, BE0083, BioXcell) and IgG2a (C1.18.4, BE0085, BioXcell). Antibodies used for in vivo leukocyte cell depletion were: anti-mouse CD4 (clone GK1.5, BP0003-1, BioXcell), anti-mouse CD8 (clone 2.43, BP0061, BioXcell), anti-mouse NK1.1 (clone PK136, BE0036, BioXcell), and control anti-keyhole limpet hemocyanin (clone LTF-2, BP0090, BioXcell). Antibodies used for protein quantification for ELISAs were mouse monoclonal anti-His (His-Tag mAb, 70796, EMD-Millipore), and biotinylated mouse anti-rat CD4 (clone OX68). OX68 was purified from the spent tissue culture supernatant from the hybridoma which was a kind gift of Professor Neil Barclay (University of Oxford). Secondary antibodies used were goat anti-mouse alkaline phosphatase conjugated secondary (A3562, Sigma-Aldrich) and rabbit anti-bovine alkaline phosphatase conjugated secondary (A0705, Sigma-Aldrich). Mouse antibody isotypes were determined using the mouse monoclonal antibody isotyping kit (ISO2-KT Sigma-Aldrich).
Validation	The specificity of the monoclonal antibodies to IFX, including the isotyped switched 8E12 mAb were validated by ELISA and their

affinities quantified by surface plasmon resonance, as described in the study. The rabbit polyclonal antibody to the entire ectodomain of IFX was validated by ELISA against the recombinant IFX ectodomain. The mouse monoclonal antibodies used for cell depletions have been routinely used for this purpose and references describing their use can be found on the supplier's website (https://bxcell.com).

Eukaryotic cell lines

Policy information about cell lines

Cell line source(s)	HEK293E (Durocher et al. 2002) or HEK293-6E (Loignon et al. 2008) were kindly provided by Yves Durocher (NRC, Montreal).
Authentication	Neither the HEK293 or HEK293-6E cell lines were authenticated.
Mycoplasma contamination	HEK293 and HEK293-6E cell lines were regularly tested for mycoplasma (Surrey Diagnostics, UK) and found to be negative.
Commonly misidentified lines (See ICLAC register)	No commonly misidentified cell lines were used in this study.

Animals and other organisms

Policy information about studies involving animals; ARRIVE guidelines recommended for reporting animal research

Laboratory animals	The animals used in this study were 6 to 8 week old female Mus musculus strain BALB/c which were obtained from a breeding colony at the Research Support Facility, Wellcome Sanger Institute. Animals were maintained on a 12-hour light/dark cycle at a constant temperature of 23oC.
Wild animals	No wild animals were used in the study.
Field-collected samples	No field collected samples were used in the study.
Ethics oversight	All animal experiments were performed under UK Home Office governmental regulations (project licence numbers PD3DA8D1F and P98FFE489) and European directive 2010/63/EU. Research was ethically approved by the Sanger Institute Animal Welfare and Ethical Review Board.

Note that full information on the approval of the study protocol must also be provided in the manuscript.